Manuscript Click here to access/download;Manuscript;L4_manuscript.docx

Predicted shifts in bacterial and algal contributions to DMSP and DMS dynamics during a coastal spring–summer bloom

Xiao-Yu Zhu[1,2,3], Frances E. Hopkins[4]*, Ruth Airs[4]*, Claire E. Widdicombe[4], Bethany Wilkinson[4], Glen A. Tarran[4], E. Malcolm S. Woodward[4], Ornella Carrión[1,2,3], Andrew R. J. Curson[1,3], Qianyao Ma[5], Libby Hanwell[1,3], Gui-Peng Yang[5], Joseph A. Christie-Oleza[6], David J. Lea-Smith[1,3], Xiao-Hua Zhang[5], and Jonathan D. Todd[1,2,3,5*]

[1]School of Biological Sciences, University of East Anglia, Norwich Research Park, Norwich, UK.

[2]Quadram Institute, Rosalind Franklin Road, Norwich Research Park, Norwich, UK.

[3]Centre for Microbial Interactions, Norwich Research Park, Norwich, UK.

[4]Plymouth Marine Laboratory, Plymouth, UK.

[5]Frontiers Science Center for Deep Ocean Multispheres and Earth System, and College of Marine Life Sciences, Ocean University of China, Qingdao, China.

[6]Department of Biology, University of the Balearic Islands, Palma, Spain.

***Correspondence:**

Jonathan D. Todd, Email: jonathan.todd@uea.ac.uk, Tel: +44-1603-592264

Frances E. Hopkins, Email: fhop@pml.ac.uk, Tel: +44-1752-633100

Ruth Airs, Email: ruai@pml.ac.uk

Running title: Dynamics of DMSP Producing and Cycling in Coastal Seawater

Abstract

Ubiquitous marine microalgae and bacteria produce the abundant organosulfur compound dimethylsulfoniopropionate (DMSP) and/or catabolise it to climate-active gases, such as dimethylsulfide (DMS), with major consequences for global biogeochemistry and climate. However, their relative and dynamic roles in DMSP synthesis and catabolism remain poorly resolved, particularly during natural bloom events. Here, we combined metagenomics and metatranscriptomics, with measurements of intracellular/particulate DMSP (DMSPp), DMS concentrations and DMSPp production rates, as well as microscopy and flow cytometry, to predict the key microbes and enzymes driving DMSP/DMS dynamics during a spring–summer bloom in the Western English Channel. Microalgae and bacteria expressing the DMSP synthesis genes *DSYB/DSYE* and *dsyB* were likely major and significant DMSP producers, respectively, except during the largest observed DMSP spike. This spike coincided with elevated *Synechococcus* and autotrophic flagellate biomass but minimal DMSP synthesis gene expression. Axenic *Synechococcus* strains contained no detectable DMSP, implying flagellates with novel DMSP synthesis genes were likely responsible. Microbial DMSP import potential far exceeded catabolism, suggesting strong selection for DMSP uptake. Bacteria were the major predicted DMSP degraders, with DMSP demethylation potential dwarfing cleavage. However, the highest DMS concentrations were linked to *Haptophyta* expressing the DMSP lyase gene *Alma*, implying the significance of algal DMSP cleavage. Methanethiol-dependent DMS production was also likely important, with bacterial *mddH* transcripts coinciding with another major DMS spike. Overall, these results imply dynamic and

contrasting roles of microalgae and bacteria, and their pathways, in coastal DMSP/DMS and sulfur cycling.

Keywords: DMSP synthesis genes, DMSP-producing microalgae and bacteria, Coastal DMSP cycling, Microalgal blooms

Introduction

Billions of tonnes of the sulfonium zwitterion dimethylsulfoniopropionate (DMSP) are produced annually in Earth's surface oceans [1, 2] (Fig. 1). Organisms produce DMSP for its anti-stress functions (e.g., for osmoprotection and antioxidation), sulfur and carbon storage, and signalling [1]. Key DMSP synthesis genes have been identified in microalgae (*DSYB*, *DSYE*, and *TpMMT*) [3-5], some cyanobacteria (*dsyG* and *dsyGD*) [4], and heterotrophic bacteria (*dsyB*, *dsyGD*, and *mmtN*) [4, 6, 7]. Microalgae are widely recognised as the major DMSP producers in Earth's surface oceans, but intracellular/particulate DMSP (DMSPp) levels are highly variable in different taxa [8, 9]. Generally, *Haptophyta* (haptophytes) and *Dinophyta* (dinoflagellates) are high DMSP accumulators (HiDA, ≥50 mM) and contain *DSYB*, whereas *Bacillariophyta* (diatoms) are low DMSP accumulators (LoDA, <50 mM) and can contain *TpMMT* [9]. *DSYE* is found in both HiDA and LoDA algae, whilst all DMSP-producing bacteria are considered LoDA [4, 9]. DMSP-producing bacteria are likely more prominent contributors to the significant DMSP levels in marine sediments, aphotic and deep ocean environments [7, 10-12].

DMSP can be released into the environment by cell lysis and/or export (Fig. 1). Diverse organisms, including heterotrophic bacteria, phytoplankton, and macroalgae, can actively import DMSP and often concentrate it to mM cellular levels [13-18] for its anti-stress properties or for catabolism [1, 19] (Fig. 1). The known DMSP transporters are from BCCT [20] and ABC (SAR11_1336 [21] and DmpX [22]) transporter families. DMSP can be catabolised via demethylation and/or cleavage pathways by DMSP-producing and non-producing organisms [19], processes which are generally thought to be driven by bacteria [19, 23, 24]. Bacteria and microalgae can also oxidise DMSP to dimethylsulfoxonium propionate (DMSOP), which is thought to have a role in oxidative stress protection, but the biosynthesis enzymes are unknown [25].

Bacterial DMSP demethylation, initiated by DMSP demethylase (DmdA, converting DMSP to methylmercaptopropionate (MMPA)) and subsequently DmdB, DmdC, and DmdD/AcuH [26, 27], is predicted to be the dominant marine catabolic pathway [28-30], utilised for carbon and/or sulfur assimilation, and can yield the climate-cooling gas methanethiol (MeSH) [26, 27] (Fig. 1). DmdA was initially identified in Roseobacter and SAR11 [27, 30]; however, functional DmdA homologues (DmdA_like) have recently also been detected in *Vibrio*, *Psychrobacter*, and SAR92 [31, 32]. MeSH can also be generated from the demethylation of methionine (Met) through L-Met gamma-lyase (MegL) [33, 34] (Fig. 1). DMSP cleavage yields the climate-cooling gas dimethyl sulfide (DMS) plus acrylate (via Alma-family enzymes [35], DddK [16], DddL [36], DddP [37], DddQ [38], DddU [39], DddW [40], and DddY [41]), 3-hydroxypropionate (3-HP)-CoA (via DddD [42]), or acryloyl-CoA

(via DddX [43]) through nine “Ddd” DMSP lyases in bacteria and fungi or Alma-family enzymes in microalgae (Fig. 1). Most DMS generated by marine microorganisms is released into the environment where it is a signalling molecule, nutrient for methylotrophs, or transferred to the atmosphere to influence cloud formation and global sulfur cycling [19, 44] (Fig. 1). The 3-carbon co-products of DMSP cleavage can be assimilated or used to deter predators [45] (Fig. 1). Hydrogen sulfide (H_2S), MeSH, and dimethyl sulfoxide (DMSO) are also DMS biosources through bacterial, archaeal and/or algal *S*-methylation (via MddA [46, 47], MddH [48], MddM1 [49], and MddM2 [49]) or reduction (via DmsA [50, 51], DorA [52], and TorZ [53]) (Fig. 1). Conversely, DMS can be oxidised to DMSO by the multicomponent monooxygenase DsoABCDEF [54], DMS dehydrogenase DdhABC [55], and flavin-containing trimethylamine monooxygenase Tmm [56]; and degraded to MeSH by the DMS monooxygenase DmoAB [57] (Fig. 1). MeSH can be degraded to sulfane sulfur (S^0) by the bacterial MeSH oxidase MtoX [58] (Fig. 1).

Many molecular ecological studies predict key microbial DMSP producers and degraders in seawater [12, 30, 59-62] and sediment [7, 10, 11, 63], but they have notable limitations. Most lack accompanying process measurements to validate their predictions. PCR-based studies are inherently biased by the primer specificity and typically exclude eukaryotic genes due to the absence of appropriate primers. In contrast, marine metagenomic and metatranscriptomic analyses are mostly performed on size-fractionated (e.g., 0.2-3 μm and >3 μm) samples, making it difficult to directly infer the contributions of larger celled algae and bacteria. Furthermore, the important microalgal DMSP synthesis gene *DSYE* [4] had not been

discovered when many earlier DMSP cycling studies were conducted. With these limitations, there was a critical requirement to integrate multi-omics approaches with in situ process measurements to assess the potential contributions of microalgae and bacteria to DMSP production and cycling in marine environments.

In this study, surface coastal seawater was sampled from the L4 marine station (Fig. S1) in the Western English Channel (WEC) between March and July 2021, spanning reoccurring diatom (April–June) and dinoflagellate blooms (June–September) [64]. DMSPp and DMS concentrations, DMSPp production rate measurements, microscopy, flow cytometry, and multi-omics analyses on >0.2 μm samples were combined to predict the key organisms, enzymes, and pathways involved in DMSP synthesis, catabolism, and related processes at this established marine station (Tables S1 and S2).

Materials and Methods

Seawater sample collection

Seawater samples from 10 m depth were collected weekly (conditions permitting) by 10 L Niskin bottles mounted on a rosette sampler which also housed a Seabird 19+ CTD from March to July 2021 at the long-term time series station L4 in the WEC (Fig. S1, Table S1). Throughout the study, samples were consistently collected between 08:20 and 10:30 UTC, except on 21 June, when sampling occurred at 11:45 UTC.

Measurements of nutrients, temperature, dissolved oxygen, salinity, Chlorophyll a (Chl-a), and plankton abundance and biomass

Nutrient samples were collected under clean conditions, kept cool and in the dark, and returned to the laboratory in Plymouth as soon as possible. Samples were filtered through 0.2 µm Millipore Fluoropore filters, and the filtrate was analysed by a 5-channel SEAL segmented flow analyser to determine the concentrations of ammonia, nitrate, nitrite, phosphate, and silicate. Temperature, dissolved oxygen, and salinity were directly measured by a Seabird 19+ CTD and its attached sensors during seawater collection. Chl-a concentrations were determined by filtering 100 mL of seawater through 25 mm GF/F filters, extracting pigments overnight in 90% acetone at 4°C, and measuring fluorescence with a Turner fluorometer as previously described [65].

Synechococcus and heterotrophic bacterial abundances were determined by flow cytometry (BD Accuri C6 flow cytometer) as previously described [66]. *Synechococcus* cells were identified by their natural pigment fluorescence and were gated based on their characteristic combination of low side scatter, orange phycoerythrin fluorescence, and red chlorophyll fluorescence, which distinguished them from heterotrophic bacteria and eukaryotic phytoplankton. Heterotrophic bacterial cells were enumerated separately after nucleic-acid staining with SYBR Green I and were distinguished from phototrophic cells based on their green fluorescence and side-scatter signatures. Cell concentrations were calculated from the analysed sample volume. Biomass was then estimated by multiplying cell

concentrations by the mean cellular biomass (*Synechococcus*: 0.59 pg C cell^{-1}; heterotrophic bacteria: 0.019 pg C cell^{-1}) as previously described [64].

To determine the abundance of different microalgal taxa, seawater samples were fixed with acid Lugol's iodine (all taxa except coccolithophores) or neutral formaldehyde (for coccolithophores) and analysed by light microscopy using the Utermohl counting technique [67] . Taxa-specific cell biovolumes were converted to cellular biomass (pg C cell^{-1}) using previously described equations [68]. Microalgal biomass was then estimated by multiplying cell abundance by the taxa-specific cellular biomass.

DMSPp, DMS, and DMSPp production rate measurements

For the characterisation of DMS concentrations, DMSPp concentrations, and DMSPp production rates, triplicate 10 L samples were collected in autoclaved and acid-washed 250 mL glass-stoppered bottles, filled ensuring no headspace, and kept in the dark to avoid photo-oxidation in a cooler during transportation to the laboratory for analysis. DMSPp and DMS concentrations were measured by gas chromatography (GC), following methods described before [69, 70]. The DMS samples were prepared by gently filtering 5 mL of seawater through a 25 mm GF/F (glass fibre) filter and transferring to a glass purge tower, avoiding any contact with air, and immediately analysing. DMS was extracted from the 5 mL sample by purging with helium at a flow rate of 60 mL/min for 5 min, whilst cryogenically trapping the DMS in a 1/16" PTFE sample loop submerged in liquid nitrogen. After 5 min, the sample loop was submerged in boiling water to desorb the DMS on a flow of helium

carrier gas onto the GC column. For DMSPp, 7–10 mL of seawater was gravity filtered onto a 0.7 µm (nominal pore size) Whatman GF/F (25 mm diameter) to collect cells. The filter was placed in an 8 mL glass vial with 7 mL of Milli-Q water, before alkaline hydrolysis with the addition of 1 mL of 10 M NaOH solution. The sample was immediately capped, sealed, and left to rest for complete hydrolysis and equilibrium (at least 12 h) prior to analysis. For analysis, 2 mL of the supernatant was pipetted from the vial directly into the glass purge tower, and purged and cryogenically trapped, before desorption onto the GC column, as outlined for DMS.

Determination of de novo DMSP synthesis, expressed as the specific DMSP synthesis rate (µDMSP), and gross DMSPp production rates was performed as outlined before [70]. For each rate measurement, 9 × 500 mL polycarbonate bottles were filled gently by siphoning water directly from a 20 L water container. Tracer amounts of $NaH^{13}CO_3$, equivalent to ~6% of in situ dissolved inorganic carbon (DIC), were added to each 500 mL bottle. PAR (Photosynthetically Active Radiation) is routinely measured at the L4 station, but on the dates of the study, the PAR sensor was not working, so coincident data are not available. However, data from other years at this site demonstrate that PAR at 10 m depth is typically between 50–200 µE m^{-2} s^{-1}. Using this as a guide, we incubated the polycarbonate bottles for DMSP synthesis rates in a Sanyo Versatile Environmental Test Chamber, set to the temperature of the seawater at the time of collection. On sunny days, the light settings in the growth cabinet were set to 150 µE m^{-2} s^{-1}, and on cloudy days a level of 65 µE m^{-2} s^{-1} was used. Triplicate samples were taken at 0 h and then at two further time points over a 6 h period. At each time point, 250 mL was gravity-filtered

in the dark sequentially through a 3 μm membrane filter and then a 0.7 μm membrane filter. Each filter was then gently folded and placed in a 20 mL serum vial with 10 mL of Milli-Q and one NaOH pellet for alkaline hydrolysis, and the vial was crimp-sealed. Samples were stored at -20°C until analysis by proton transfer reaction mass spectrometer (PTR-MS) [71]. Calculation of μDMSP from ^{13}C incorporation into DMSPp, and conversion to gross DMSPp production rates, were performed as previously described [70]. These measurements represent DMSPp production rates (i.e., production retained in the cells) rather than total DMSP production in the system. Newly synthesised DMSP released into the dissolved pool through secretion, leakage, or grazing-related processes would not be captured by this approach. In addition, microorganisms within the surface mixed layer are naturally exposed to variable irradiance due to vertical mixing, which cannot be fully replicated under fixed light conditions in bottle incubations. Therefore, the measured DMSPp production rates should be interpreted as estimates obtained under controlled incubation conditions rather than exact in situ rates.

Amplicon, metagenomic, metatranscriptomic sequencing

For microbial/microalgal community and metabolic analysis, 3 L of seawater was filtered in triplicate for DNA and RNA extraction at each sampling date immediately on board the RV Plymouth Quest. Filtration was performed using a peristaltic pump (Watson-Marlow) with 0.22 μm polyethersulfone Sterivex filter units (Millipore). The process was completed within 2–8 hours of sampling, after which filters were immediately flash-frozen in liquid nitrogen, before being transferred to -80°C freezer. We acknowledge that the filtration period may represent a limitation for

metatranscriptomic analyses because of the rapid turnover of mRNA in natural microbial communities.

Twelve of the eighteen sampling dates were selected for downstream multi-omics analysis. Each filter was halved for parallel DNA and RNA extraction using the PowerSoil DNA Isolation Kit (Qiagen) and the Direct-zol RNA Kit (Zymo Research), respectively. For 16S rRNA amplicon sequencing, the V4 region was amplified using the 515F and 806R primers [72, 73]. All amplicons, metagenomes (total DNA), and metatranscriptomes (total RNA) were submitted to Novogene (Beijing, China) for quality control, library construction, and high-throughput sequencing on a HiSeq X Ten System (Illumina). Samples that failed to meet quality control standards were excluded from further sequencing.

Metagenomic and metatranscriptomic analyses

Raw metagenomic and metatranscriptomic data were primarily quality controlled by Fastp v0.23.2 [74]. SortMeRNA v4.3.6 [75] was further used to remove rRNA reads in metatranscriptomes. Clean reads of metagenomes or metatranscriptomes were then co-assembled for each sampling date with MEGAHIT v1.0.2 [76]. Prodigal v2.6.3 [77] and FragGeneScan [78] were used to predict genes for metagenomic and metatranscriptomic assemblies, respectively. Then, predicted genes from metagenomes and metatranscriptomes were clustered at 95% identity using CD-HIT v4.8.1 [79] to obtain the non-redundant gene catalogue. Taxonomic assignment of prokaryotic genes was conducted by the “easy-taxonomy” module in MMseq2 [80] with GTDB release 220 [81] as the reference database. Taxonomic assignment of

eukaryotic genes was conducted by Eukulele v2.0.9 [82] with PhyloDB (https://github.com/allenlab/PhyloDB) as the reference database.

The relative abundance of each gene in metagenomes and each transcript in metatranscriptomes were both estimated by the “metabat” method in CoverM v0.6.1 [83]. The average relative abundance of 10 single-copy marker genes [84] was used to normalise the gene relative abundance in metagenomes as described previously [29]. These ten marker genes were retrieved using hmmsearch v3.4.2 [85] with an e-value threshold of 1e-10. In contrast, transcript relative abundance in metatranscriptomes was normalised by the total read count of each metatranscriptome.

Analyses of community composition

Qiime2 platform [86] was used to analyse the 16S rRNA gene amplicon data. The “DADA2” plugin in Qiime2 was employed for quality filtering, denoising, chimera removal, and generation of amplicon sequence variants (ASVs). The “classify-sklearn” module in Qiime2 was used to assign taxonomy for each ASV based on the Silva v138.1 database [87]. Phyloflash v3.4.2 [88] was applied to determine the prokaryotic community from metagenomes based on 16S rRNA gene reads with the Silva v138.1 [87] as the reference database. For the microeukaryotic community, we retrieved the 18S rRNA gene reads from metagenomes by Bowtie2 [89] and assigned taxonomy for each read using IDTAXA [90]. Both the identification and taxonomic assignment of 18S reads used the PR2 v4.13 as the reference database [91]. We filtered out non-protistan sequences, defined as those that were

assigned to the *Metazoa*, *Embryophyta*, and *Fungi*, before downstream analyses. Taxonomic profiles based on metatranscriptomic reads were analysed using Kraken2 [92] with the NCBI nr database as the reference database. Metatranscriptomic reads belonging to *Chordata*, *Arthropoda*, *Streptophyta*, *Mollusca*, and *Virus* were excluded. Downstream comparison analyses of microalgal and bacterial community compositions were performed with Microeco v1.14.0 [93].

Metagenome assembled genome (MAG) recovery

The co-assembly contigs of each sampling date were individually imported to Semibin2 [94] to recover bacterial and archaeal MAGs. Then, MAGs from every sample were dereplicated using dRep v2.3.2 [95]. Genome completeness and contamination were estimated by CheckM v1.0.12 [96]. Only MAGs with medium to high quality (completeness ≥70%, contamination ≤5%) were retained for downstream analysis. Taxonomic assignment of each genome was determined by the "classify_wf" module of GTDB-Tk v1.7.0 [81]. The MAG tree was also inferred by GTDB-Tk v1.7.0 [81] using the "infer" module and was then visualised in ChiPlot [97]. Gene prediction and annotation of each MAG was performed by Prokka v1.12 [98]. The relative abundance/expression of MAGs in metagenomes/metatranscriptomes were estimated using the "relative abundance" method in CoverM v0.6.1 [83].

Identification of DMSP/DMS/MeSH metabolism related genes

Enzymes assigned with Kyoto Encyclopedia of Genes and Genomes (KEGG) Orthology IDs (i.e., MegL, DsyB, DSYE, DsyGD, MmtN, DddD, DddX,DddL, DddQ,

DddP, DddW, DddY, DmdA, DmdB, DmdC, DmdD, AcuH, TorZ, DorA, DmsA, DdhA, Tmm, DmoA, MtoX, and MddA) were annotated by BlastKOALA [99]. Because DddL and DddQ, as well as TorZ and DorA, share identical KO IDs, they were grouped as DddL/Q and TorZ/DorA in subsequent analyses. BCCT transporters were annotated by DIAMOND BLASTP [100] against the TCDB database using an e-value threshold of 1e-10 [101]. The remaining enzymes (i.e., DSYB, DsyG, TpMMT, DmpX, SAR11_1336, Alma, DddK, DddU, DmdA_like, DsoB, MddH, MddM1, and MddM2) were identified by DIAMOND BLASTP [100] against their ratified sequences. Only homologues with ≥40% amino acid identity, ≥70% subject coverage, and ≥70% query coverage relative to ratified sequences were retained. For DmdA_like, DddK, MddH, and TpMMT, a set of previously identified non-homologues were included as negative reference sequences in the DIAMOND BLASTP analyses. The KO IDs and sequences of all these enzymes are available in our custom database (https://github.com/zhuxiaoyu123/DMSP-database).

For genes identified by DIAMOND BLASTP against the ratified sequences, we evaluated the sensitivity of the observed relative transcript abundance patterns to the sequence identity threshold by repeating the analysis using the threshold applied in the main analysis (40%), a more permissive threshold (30%), and a more stringent threshold (50%). Overall, the relative transcript abundance patterns were highly consistent across the three cutoffs (Fig. S2), indicating that the main conclusions were robust and not strongly influenced by the choice of sequence identity cutoff.

323 **Intracellular DMSP measurements of *Synechococcus* spp.**

324 Axenic cultures of marine *Synechococcus* strains WH7803, WH7805, WH8102, and
325 CC9311 were routinely grown in ASW medium [102] using optimal growth conditions
326 previously described [103]. For each strain, 100 mL mid-exponential phase culture
327 was harvested by gentle centrifugation (3,000 *g* for 15 min at 20 ºC) and
328 resuspended in 100 mL of nitrogen-depleted ASW medium. Cultures were pre-
329 starved for nitrogen for 24 h under optimal conditions (22°C at a light intensity of 10
330 µE m^{-2} s^{-1} with orbital shaking at 140 rpm). Subsequently, 12 mL aliquots of each
331 culture were transferred into six 50 mL vented-cap culture flasks (GRYNIA). To three
332 flasks, 120 µL of 880 mM $NaNO_3$ was added (nitrogen-replete condition), whereas
333 the remaining three flasks received 120 µL of Milli-Q water (nitrogen-depleted
334 condition). All cultures were then incubated under optimal conditions for three days
335 after which cell concentrations were measured by flow cytometry (Becton Dickinson
336 FACS-Verse cytometer) as previously described [104] and 10 mL of each culture
337 was pelleted by centrifugation (4,000 *g* for 10 min at 4 ºC) and immediately stored at
338 -20 ºC for subsequent DMSP analysis.

339

340 Pelleted *Synechococcus* cells (between 1.5×10^9 and 1.7×10^{10} cells per pellet)
341 were resuspended in 200 µL 50 mM Tris-HCl, 200 mM NaCl buffer (pH 7.5),
342 transferred to a 2 mL glass GC vial and 100 µL 10 M NaOH was added (for alkaline
343 lysis of DMS from DMSP) before immediately crimping the vial. Vials were incubated
344 at 22°C in the dark for >6 hours and then headspace DMS was measured by gas
345 chromatography as previously described [3]. DMSP standards were analysed in the

same way and DMS peak areas were used to determine DMSP concentrations in the *Synechococcus* cells. None of the *Synechococcus* samples gave DMSP above the detection limit of the instrument (0.015 nmol DMSP in 300 µL sample or 0.05 µM). Based on the cell numbers in the samples and assumed *Synechococcus* cell volume (3 μm^3) [105], this would mean that any DMSP produced by these strains would be at estimated intracellular concentrations of less than 0.3–3.3 µM or 0.9–10 zmol per cell.

Statistical analyses

Pairwise Spearman correlations were analysed and plotted using the LinkET (https://github.com/Hy4m/linkET) package in R. Spearman rank correlation is a non-parametric approach that does not assume normally distributed data or linear relationships and is less sensitive to outliers. *P* values were adjusted for multiple testing using the Benjamini–Hochberg method to control the false discovery rate.

Results

Microbial community analysis of the L4 spring bloom 2021

The 2021 spring-summer bloom at station L4 consisted of a pre-bloom phase (23 March–6 April) with low microalgal biomass, a diatom (*Bacillariophyta*)-dominated phase (13 April–25 May), and a dinoflagellate (*Dinophyta*)-bloom phase (2 June–19 July) (Fig. 2a, Figs. S3 and S4). A *Synechococcus* bloom was also observed on 28 June, with biomass comparable to that of autotrophic dinoflagellates (Fig. 2a and b). Heterotrophic bacteria showed increased biomass after the late diatom-bloom, when diatoms had likely senesced and released intracellular organic matter (Fig. 2c).

Community composition analyses (by 16S rRNA gene amplicon, metagenomic, and metatranscriptomic sequencing) largely supported these observations, and revealed increased relative abundance of *Pseudomonadales*, *Flavobacterales*, and *Rhodobacterales* in the two bloom phases compared to the pre-bloom phase (Fig. 2d, Figs. S5–S7).

DMSPp and DMS concentrations in L4 samples

The pre-bloom phase showed the lowest observed DMSPp, DMS and Chl-a concentrations, and DMSPp production rates (Fig. 2e). The onset of the diatom bloom led to a rapid increase in DMSPp concentration, which was relatively stable throughout both bloom phases, except for a small spike during the diatom bloom (20 April, 70.4 nM) and a larger spike during the dinoflagellate bloom (28 June, 164.76 nM). Although total DMSPp production rates slightly increased during the dinoflagellate bloom compared to the diatom bloom phase, the contribution from small microalgae and free-living bacteria (0.7–3 μm) increased significantly and far exceeded that of larger microalgae and particle-associated bacteria (>3 μm) in the early and middle phases of the dinoflagellate bloom (Fig. 2e), suggesting that smaller microbes dominated DMSP production during this period. There was no significant correlation between DMSPp and Chl-a concentrations in the L4 samples (Fig. 3a), implying that the microalgal community were predominantly not HiDA and thus had likely low DMSPp:Chl-a ratios. This could not be corroborated by taxonomy because the dominant diatoms and dinoflagellate species (Fig. S4) had not previously been studied for DMSP production [9]. Furthermore, surface ocean Chl-a is only known as a good predictor of DMSP levels when HiDA microalgae are

prominent [106-108]. In accordance with this, far higher DMSPp:Chl-a ratios (51.06 versus 25.09 on average) were observed during the dinoflagellate bloom compared to the diatom bloom samples (Fig. 2e), consistent with dinoflagellates and diatoms generally being HiDA and LoDA, respectively [9].

Correlation analysis of environmental parameters, microbial taxa, and DMSPp/DMS levels

DMS concentrations (1.78–27.41 nM) positively correlated with DMSPp levels (Spearman's rho = 0.66, $P < 0.05$), and were generally higher during the two bloom phases, but were always present at much lower levels than its likely DMSP precursor (20.51–164.76 nM) (Figs. 2e and 3a). DMSPp levels showed a significant negative correlation with ammonia levels (Spearman's rho = -0.64, $P < 0.05$, Fig. 3a), consistent with DMSP-producing algae and bacteria shifting metabolism to produce more nitrogen-independent osmolytes, such as DMSP, in response to nitrogen limitation [6, 9]. DMSP levels were also positively correlated with temperature and negatively correlated with silicate and phosphate (Fig. 3a). This pattern is likely explained by higher DMSPp concentrations associated with greater biomass of DMSP-producing phytoplankton at elevated temperatures, which in turn may contribute to the rapid drawdown of nutrients such as silicate and phosphate. Supporting this interpretation, all microalgal groups that were positively correlated with temperature were negatively correlated with these nutrients at L4 (Fig. 3b).

Correlations between DMSPp and various taxonomic groups were examined to explore potential associations between plankton groups and DMSP production (Fig.

3b). All significant correlations were observed in microalgal groups, supporting their well-established role in DMSP synthesis [9, 106]. Autotrophic flagellates (too small to be identified by microscopy) and auto-/mixotrophic *Dinophyta* displayed the strongest relationships with DMSPp (Spearman's rho = 0.81, $P < 0.05$), followed by *Haptophyta* (Spearman's rho = 0.69, $P < 0.05$) (Fig. 3b). Given that *Haptophyta* and *Dinophyta* are commonly considered as HiDA [9], these associations suggest that they may contribute to DMSP production at L4. No significant correlations were observed between DMSPp and other plankton groups. However, given the high biomass of certain groups (e.g., diatoms, *Synechococcus*, and heterotrophic bacteria; Fig. 2a–c) and/or the high DMSP synthesis potential of others (e.g., *Cryptophyta* and *Chlorophyta* [9]), their contributions to total DMSPp cannot be excluded.

Correlations between DMS and various taxonomic groups were examined to explore potential associations between plankton groups and DMS dynamics (Fig. 3b). Only *Haptophyta* showed a positive correlation with DMS (Spearman's rho = 0.76, $P < 0.05$). No significant correlations were observed for other groups, possibly reflecting substantial variability in DMS production capacity and associated pathways among plankton taxa, as well as the fact that DMS concentrations represent the net balance between production and loss processes (e.g., air–sea exchange and photochemical or biological oxidation) [44]. Therefore, metagenomic and metatranscriptomic analyses of the presence, expression, and taxonomic affiliation of known DMSP/DMS metabolism-related genes may better predict the organisms and pathways influencing DMSP and DMS dynamics at L4.

Microalgae and bacteria were respectively predicted as dominant or significant DMSP producers

Metagenomics and metatranscriptomics were performed on >0.22 μm fractionated samples to characterise the genetic potential and transcriptional profiles of bacteria and larger microalgae. Genes involved in DMSP/DMS/MeSH-related metabolism were identified and quantified in metagenomes (indicated as % of prokaryotes), metatranscriptomes (represented by transcripts per million reads “TPM”), and MAGs (Figs. 4–7, Figs. S8–S10, Tables S3–S7). Eukaryotic genes were sparsely detected in our metagenomic samples, likely because predicting eukaryotic genes from metagenomic assemblies remains challenging owing to their complex gene structures (e.g., introns and exons) and the prokaryote-focused bias of many gene-prediction tools [109]. They were therefore excluded from the metagenomic analyses.

Metagenomic analysis of samples from station L4, like that of the global surface ocean [4, 110], predicted that only a small proportion (0.53% of prokaryotes on average; 0.52% with *dsyB* and 0.01% with *mmtN*) of L4 prokaryotes could produce DMSP (Fig. S8, Table S3). Consistently, only 8 of 260 MAGs were predicted with *dsyB* and none had *mmtN* or *dsyG/GD* genes (Fig. 4, Table S7). *DsyB* genes detected in metagenomes were mainly affiliated with members of the *Pseudomonadota*, particularly *Pseudomonadales*, *Burkholderiales*, *Rhodobacterales*, and *Thalassobaculales*, with additional sequences assigned to

460 *Acidimicrobiales* (*Actinobacteriota*) (Fig. S8), suggesting that the potential for DMSP
461 production was distributed across diverse marine bacterial taxa.

462

463 By metatranscriptomic analysis, we estimated the transcript abundance of eukaryotic
464 and prokaryotic DMSP synthase genes. Eukaryotic synthase gene transcripts were
465 more abundant than their prokaryotic counterparts (1.25 versus 0.14 TPM). Although
466 transcript abundance is not a direct measure of enzymatic activity or process rates,
467 the higher abundance of eukaryotic DMSP synthase transcripts, together with the
468 positive correlations between DMSPp concentrations and the biomass of several
469 phytoplankton groups (Fig. 3b), and the high intracellular DMSP concentrations
470 typically found in microalgae [9], supports the interpretation that microalgae were
471 likely major DMSP producers at L4. *DSYB*, mainly from *Dinophyta* and *Haptophyta*,
472 was the most highly expressed known DMSP synthesis gene across all L4 samples
473 (0.98 TPM average, Fig. 5). Algal *DSYE* transcripts (0.24 TPM), largely from
474 *Chlorophyta*, *Bacillariophyta*, and *Haptophyta*, were always much less prominent
475 than for *DSYB*, but generally more abundant than for bacterial *dsyB* (0.14 TPM)
476 (Table S5). Algal *TpMMT* (0.01 TPM) and bacterial *mmtN* (0.001 TPM) transcripts
477 were far less frequent, consistent with global surface ocean analysis [4, 111] (Fig. 5).
478 Although microalgae accounted for the majority of DMSP synthesis transcripts,
479 bacterial *dsyB* transcripts, mainly from *Burkholderiales* and *Pseudomonadales*, were
480 consistently detected and in some samples reached levels comparable to algal
481 *DSYE* (Fig. 5), suggesting that bacteria may represent significant contributors to
482 DMSP synthesis. These data extend the potentially important role of bacteria in
483 DMSP synthesis beyond previously reported aphotic and sediment environments [7,

12], showing that bacteria may also contribute significantly to DMSP synthesis in sunlit seawater alongside microalgae.

Cumulatively, DMSP synthase gene transcripts, particularly *DSYB*, were more abundant during the diatom bloom versus the dinoflagellate bloom (Fig. 5a). However, DMSPp concentrations remained broadly comparable between the two phases, except for a pronounced spike on 28 June. In addition, total DMSPp production rates were generally higher during the dinoflagellate bloom (Fig. 2e). Moreover, no significant correlations were observed between DMSP synthesis gene transcript abundance and DMSPp/DMS concentrations or DMSPp production rates (Fig. S11). These discrepancies could reflect shifts in the composition of DMSP-producing taxa between the two bloom phases, with *DSYB* transcripts from the haptophytes *Phaeocystis* and *Chrysochromulina*, and the dinoflagellate *Heterocapsa* being more abundant during the diatom-dominated phase (Fig. 5b). Conversely, *DSYB* transcripts from the dinoflagellate *Ceratium* were more abundant during the dinoflagellate bloom. This temporal succession of *DSYB*-expressing taxa may indicate a shift among *DSYB*-expressing taxa carrying isoforms with potentially different enzymatic properties, potentially decoupling *DSYB* transcript abundance from DMSPp concentrations and DMSPp production rates (Fig. 5a, Fig. S11). *DSYE* transcript abundance did not change significantly during the blooms, but diatom *DSYE* and *TpMMT* transcripts, although low (< prokaryotic gene transcripts), were generally more prominent during the diatom bloom (Fig. 5a). Furthermore, all detected eukaryotic synthesis transcripts were not from the dominant predicted microalgal genera observed in the L4 samples (Fig. S4), implying that many of the

algal taxa were either (a) not producing DMSP (i.e., not expressing their synthesis genes), (b) utilising unknown DMSP synthesis genes (e.g., from the decarboxylation pathway in *Crypthecodinium cohnii* [112]), or (c) lacked the capacity for DMSP production. Cases (a) and (c) would highlight the potential contribution of subdominant taxa and potentially HiDA dinoflagellates, haptophytes and chlorophytes, and to a lesser extent LoDA bacteria, in DMSP production during the spring microalgal bloom at L4.

The highest DMSPp and DMSPp:Chl-a levels, observed in the 28 June samples, coincided with the lowest abundance of known DMSP synthesis gene transcripts. This peak aligned with a substantial increase in *Synechococcus* abundance (Fig. 2b), a predicted LoDA [9] previously estimated to accumulate 2–21% of DMSP in the WEC [113]. *Synechococcus* spp. are known to import DMSP from the environment [17], but their ability to produce DMSP remains uncertain. Low intracellular DMSP levels (0.03–0.7 mM) have been reported in two non-axenic cultures [114], whereas another study found no detectable DMSP in eleven non-axenic *Synechococcus* samples [9]. To establish if *Synechococcus* can synthesise DMSP, we analysed axenic cultures of four species that were phylogenetically close to L4 *Synechococcus* (Fig. S12). These strains were grown in artificial seawater media under nitrogen replete or depleted conditions. Significantly, none of these cyanobacteria accumulated DMSP above the detection limit of the GC instrument, irrespective of nitrogen levels, which are known to regulate DMSP production in many producers [1] (see methods). If DMSP was present in these cyanobacteria it would, at best estimate, be equivalent to 0.3–3.3 µM or 0.9–10 zmol per cell, see

methods, indicating that these *Synechococcus* are unlikely to be major contributors to DMSP levels in the L4 samples. However, it is possible that the exact *Synechococcus* populations at station L4, which were not cultured here, possess unknown DMSP synthesis genes and accumulated higher DMSP levels than we observe in the closely related tested strains. The DMSPp spike on 28 June also coincided with a peak in abundance of autotrophic flagellates (Fig. 2a), which showed significant correlation with DMSPp (Spearman's rho = 0.81, $P < 0.05$, Fig. 3b). Thus, rather than *Synechococcus*, it is more likely that some of these small microalgae present were HiDA with unknown DMSP synthesis genes, as is the case for the dinoflagellate *C. cohnii* that utilises the decarboxylation pathway for DMSP synthesis [112], and were responsible for this larger DMSPp spike.

Bacteria and microalgae were respectively predicted dominant or significant DMSP degraders

Bacterial *dmdA/dmdA_like* genes (37.3% of prokaryotes) and transcripts (13.6 TPM) were more abundant than *ddd* genes (22.6% of prokaryotes) and their transcripts (5.5 TPM) in L4 samples (Fig. 6a, Fig. S9a, Tables S3 and S5), consistent with previous reports in the global ocean [29, 30] and supporting the dominant role of bacterial demethylation in DMSP catabolism across diverse marine environments [28]. The two main lyase genes at L4 were *dddP* and *dddU*, with the latter previously shown not to be prominent in the global surface open-ocean [29], indicative of differences in bacterial community composition between open-ocean and coastal waters. Although fungi contributed significantly to ocean biomass (9/44 of bacterial biomass in open-ocean) [115], their *dddP* [37] and *dddW* [116] genes

were not detected in our metatranscriptomes, suggesting their minimal role in L4 DMSP cycling.

Bacteria were predicted as the dominant DMSP degraders based on far higher prokaryotic *dmdA/dmdA_like* (13.6 TPM) and *ddd* relative transcript abundances (5.5 TPM) compared to eukaryotic *Alma* (0.87 TPM) in all samples (Fig. 6a, Table S5). The *dmdA/dmdA_like* and *ddd* genes were largely from *Rhodobacterales* (mainly *Amylibacter* and *Planktomarina*) (Fig. 6a and b), whose biomass greatly increased during both blooms (Fig. 2c and d) and whose relative abundance was previously shown to strongly correlate with HiDA microalgae in coastal seawaters [117]. Among the 31 *ddd/dmdA*-containing *Rhodobacterales*, 67% (21) encoded both *ddd* and *dmdA/dmdA_like* genes, and 58% (18) harboured multiple *ddd* and/or *dmdA/dmdA_like* genes (Fig. 4). These proportions were markedly higher than those observed in the 33 *ddd/dmdA*-containing MAGs from other taxa, of which 27% (9) encoded both genes and 12% (4) contained multiple *ddd* and/or *dmdA/dmdA_like* genes. In addition, compared with these 33 MAGs from other taxa, the *ddd/dmdA*-containing *Rhodobacterales* were also enriched in the DMS oxidation gene *tmm* and the MeSH degradation gene *mtoX* (Fig. 4). Together, these results suggest that *Rhodobacterales* may play a relatively important role in DMSP cleavage and demethylation, as well as in downstream DMS and MeSH metabolism. Other *dmdA* or *ddd* genes were mainly from *Pseudomonadales*, *Pelagibacterales* and PS1 or *Pelagibacterales* and *Rhodospirillales*, respectively (Fig. 6a and b).

578 Alma-family DMSP lyase gene transcripts, mainly from *Haptophyta* and *Dinophyta*,
579 were always less abundant than for *ddd*, except on 20 April and 4 May, which
580 corresponded with a minor and the largest observed DMS spikes in the diatom
581 bloom, respectively (Fig. 6a). Furthermore, *Haptophyta* biomass was shown to have
582 strong relationships with DMS (Spearman's rho = 0.76, $P < 0.05$, Fig. 3b). The minor
583 DMS peak was associated with *Dinophyta* and the largest with *Haptophyta*,
584 predominantly *Phaeocystis* (Fig. 6a and b), a genus often associated with active
585 DMSP cleavage [118, 119]. Bacterial *ddd* transcripts were barely detected in these
586 two samples, suggesting that microalgae played a key role not only in DMSP
587 synthesis but also in its cleavage. Moreover, *Dinophyta*-derived *Alma* genes were
588 consistently expressed across the spring bloom (Fig. 6b). These findings support a
589 previous study, which proposed that bacteria-mediated DMS production alone could
590 not account for the high DMS concentrations seen in surface seawaters [107].

591 **MeSH may be an important precursor of DMS at L4**

592 We did not see any co-variation between DMS concentration and DMSP lyase
593 transcript relative abundance (Fig. S11). This was likely due to variability in the
594 enzymatic efficiencies of the different known DMSP lyases [120], the activity of as
595 yet unidentified DMSP lyases, or of other biological DMS generating or catabolic
596 pathways [44] (Fig. 1), in combination with multiple dynamic and variable non-
597 biological loss pathways for DMS from the surface ocean (e.g., ventilation to the
598 atmosphere via the sea-air flux and photo-chemical reactions) [44]. Indeed, the
599 second largest observed DMS spike corresponded to the 28 June sample, with the
600 highest DMSP level, lowest DMSP synthesis potential (described above), and,

significantly, one of the lowest observed levels of *ddd/Alma* transcripts. Thus, other known DMS production genes were examined in the L4 samples (Fig. 6a and b, Fig. S9a and b). The 28 June sample exhibited the highest abundance of *mdd* genes/transcripts, whose products convert H_2S and MeSH to DMS [46-48] (Fig. 1). These *mddH* gene products, primarily from SAR86 and *Pseudomonadales*, may have contributed to the second highest observed DMS peak in the L4 samples. Excepting the 28 June samples, *mdd* genes and transcripts were generally less abundant than those for *ddd* genes (17.2% versus 22.6% of prokaryotes; 4.7 versus 5.5 TPM) but even these levels were clearly sizable and imply they played a significant role in sulfur cycling at L4 (Fig. 6a, Fig. S9a, Tables S3 and S5). *mddH* genes/transcripts were far more abundant than *mddA* (14.4% versus 2.7% of prokaryotes; 4.0 versus 0.6 TPM), which is thought to be more prominent in terrestrial environments [46-48]. The genetic potential for MeSH production from DMSP demethylation and Met lysis as well as MeSH degradation is extensive in L4 samples (Figs. 1 and 6a, Fig. S13, Tables S3 and S5). Given this prediction and that H_2S concentrations are often below detection limits in well-oxygenated surface ocean samples [121, 122], MeSH was therefore likely the key Mdd substrate, suggesting significant potential for MeSH-dependent DMS production in this marine environment.

DMSO reductase genes and transcripts, which encode enzymes that reduce DMSO to DMS, were also seen in the L4 samples but at levels lower than for DMSP cleavage and H_2S/MeSH-dependent DMS production pathways (0.1% of prokaryotes; 0.01 TPM) (Fig. 6a and b, Fig. S9a and b, Tables S3 and S5). This is

consistent with a previous finding at L4, where >94% of DMSO was dissimilated to CO_2 [123].

DMS levels are also influenced by its consumption, not measured here. Nevertheless, microbial DMS oxidation may play an important role in DMS removal in L4 samples, supported by the notable mean relative abundance (10.9% of prokaryotes) and relative expression (2.8 TPM) of *tmm* genes (Fig. 6a, Fig. S9a, Tables S3 and S5). Reduced *tmm* expression observed in the 20 April and 4 May samples may have further contributed to the elevated DMS concentrations on those dates (Fig. 6a).

Bacterial DMSP import potential outweighs catabolism

The putative DMSP transporter genes *BCCT*, *SAR11_1336*, and *dmpX* were predicted in 44.1%, 8.0%, and 22.9% of prokaryotes, respectively. Collectively, these genes were more prevalent than known bacterial DMSP cleavage (22.6%), demethylation (37.3%), and synthesis (0.53%) genes (Fig. S9a, Table S3). Their combined transcript abundance (78.6 TPM) was also markedly higher than that of bacterial DMSP cleavage (5.5 TPM), demethylation (13.6 TPM), and synthesis (0.14 TPM) genes (Fig. 7a, Table S5). This pattern is unsurprising given some bacteria that do not catabolise DMSP can still use it for osmoprotection [124, 125]. Only DmpX is known to be highly specific for DMSP import, whereas BCCT and SAR11_1336 transporters can also import other compounds such as betaines [20, 21]. Therefore, the high abundance of these transporter genes may reflect a broader

compatible solute uptake capacity in these bacteria rather than DMSP-specific import alone.

Although dissolved DMSP (DMSPd), rather than DMSPp, is the form directly available for transport, DMSPd and DMSPp often exhibit broadly similar distribution patterns in marine environments [60, 106]. In L4 samples, intracellular DMSPp concentrations broadly covaried with transcripts of putative DMSP transporter genes, primarily affiliated with predicted DMSP-degrading Pelagibacterales, Rhodobacterales and Pseudomonadales (Fig. 7a), suggesting that DMSP availability may shape microbial osmolyte uptake dynamics. ABC transporters (*SAR11_1336* and *dmpX*) exhibited lower relative gene abundance but significantly higher transcript levels compared to *BCCT* (Fig. 7a, Fig. S10a). This may reflect greater transcriptional investment in the ABC transport systems by their host strains, potentially enabling them to compete more effectively for available DMSP. Consistently, *Pelagibacter*, *Pseudothioglobus*, and *Amylibacter*, three predicted DMSP degraders at L4 (Fig. 6), encoded fewer ABC-family DMSP transporter genes than DMSP catabolic genes (Fig. S10c), but showed substantially higher expression of ABC-family DMSP transporter genes than of DMSP catabolic genes (Fig. 7c). Although this pattern was not observed in the other two predicted DMSP degraders, *Luminiphilus* and *Planktomarina*, the relative transcript abundances of their DMSP transporter genes were higher than those of their DMSP catabolic genes in most samples. These results further imply the importance of DMSP import and intracellular accumulation for catabolism and potentially as an anti-stress compound.

Discussion

This study uniquely uses molecular approaches (metagenomics and metatranscriptomics) combined with direct measurements of in situ chemical and biological variables and process measurements to predict the key microalgae and bacteria involved in DMSP synthesis and catabolism in temperate coastal surface waters during a spring microalgae bloom.

Microalgae were inferred as the primary DMSP producers in the WEC coastal waters, due to their strong correlations to DMSPp concentration (Fig. 3b), and high expression of *DSYB*, particularly from HiDA dinoflagellates and haptophytes (Fig. 5). Even though diatoms (LoDA) were abundant, notably through the diatom bloom phase (Fig. 2a), their contribution to DMSP production was likely limited as indicated by relatively low expression of diatom *DSYE* and *TpMMT* genes (Fig. 5). These data were consistent with HiDA abundance/activity, rather than total microalgal abundance, determining DMSPp production rates in the surface ocean [9, 108]. Bacteria are considered as important DMSP producers in aphotic marine waters and sediments with negligible production from microalgae [7, 12, 106]. Unexpectedly, bacteria, particularly *Pseudomonadales* and *Burkholderiales* with *dsyB*, were likely significant contributors to total DMSP levels, with *dsyB* transcripts generally more abundant (approximately 10% of total DMSP synthesis gene transcripts and 14.1% of eukaryotic *DSYB* transcripts) than algal *TpMMT*, and sometimes comparable to *DSYE* (Fig. 5, Table S5). Although the enzymatic efficiency of DsyB is slightly lower than DSYB [120], their substantial expression suggests a potentially important role

693 for LoDA bacteria in DMSP production. Given the minuscule DMSP amounts axenic
694 *Synechococcus* strains potentially accumulated, they were unlikely to be important
695 DMSP producers at L4 despite their notable biomass (Fig. 2b) and previous reports
696 of DMSP production [113, 126]. *Synechococcus* are much more likely significant
697 importers and accumulators of DMSP [127] because they contain BCCT family
698 transporters (Fig. S14), are not thought to catabolise DMSP and lack all known
699 primary DMSP catabolic enzymes.

700

701 In contrast to algal-driven DMSP synthesis, bacteria, particularly *Rhodobacterales*,
702 *Rhodospirillales* and *Pelagibacterales* with *dmdA/dmdA_like*, *dddP* and/or *dddU*,
703 were predicted as the major DMSP degraders in L4 coastal waters (Fig. 6a), as
704 previously suggested in the global ocean [28-30]. Consistent with previous
705 studies [28-30], bacterial-driven DMSP demethylation potential was always far
706 greater than DMSP cleavage potential and was relatively consistent between
707 samples. DMSP cleavage was also predominantly predicted to be bacterial, with only
708 2 of 12 samples exhibiting higher cleavage potential in DMSP-producing microalgae,
709 primarily *Haptophyta*, than bacteria (Fig. 6a). It is unclear why these microalgae in
710 the 20 April and 4 May samples likely preferentially cleaved intracellular DMSP,
711 generating cleavage products that may deter grazers [128, 129], attract heterotrophic
712 microbes [130, 131], or attract micropredators and the predators of those
713 micropredators [132]. Nevertheless, these two algal events displayed significant
714 spikes in DMS levels, highlighting the importance of both microalgae and bacteria in
715 DMSP cleavage, but also the more dynamic nature of the former. In addition to
716 DMSP, MeSH was also a likely alternative DMS precursor. This was supported by: (i)

717 significant expression of *mdd* (largely *mddH*), which in some cases (e.g., 28 June)
718 exceeded those of DMSP lyase genes and coincided with a pronounced DMS spike
719 (Fig. 6a); (ii) a high predicted potential for MeSH production via DMSP demethylation
720 and Met cleavage (Fig. S13); and (iii) the widespread presence of MeSH in the
721 global ocean [133, 134]. In contrast to Mdd pathways, DMSO was likely a less
722 significant biological source of DMS, indicated by the low observed DMSO reductase
723 expression levels (Fig. 6a) and previous observations [123].

724

725 The reason for consistently lower expression levels of DMSP synthesis genes
726 compared to those for DMSP catabolism and import, observed across all L4 samples
727 and in previous studies on other marine environments, remains unclear. One
728 possibility is that transcript abundance may not accurately reflect enzyme abundance
729 or activity. Additionally, DMSP synthesis is known to be tightly regulated by
730 environmental conditions [9], and bacterial DMSP synthesis genes are typically
731 restricted to a narrower range of taxa than for DMSP import and catabolism, which
732 are widespread among marine bacteria [1, 6, 7, 19, 20, 22-24] and support key
733 cellular functions such as growth, sulfur and carbon assimilation, and stress
734 protection [19]. DMSP transporter genes were expressed at higher levels than those
735 for catabolism in predicted DMSP degrading bacteria, including *Pelagibacter*,
736 *Amylibacter*, *Luminiphilus, Pseudothioglobus*, and *Planktomarina* (Fig. 7c, Fig. S9c).
737 This suggests a requirement to concentrate DMSP within the cell, likely for stress
738 protection and subsequent catabolism, especially given the high K_m values of the
739 associated catabolic enzymes [120].

Although our multi-omics approach enabled detailed functional and taxonomic predictions of DMSP production, import and cycling, we acknowledge several limitations. Transcript abundance does not directly reflect protein levels or enzymatic activity. Furthermore, there is still significant work required to establish the functional divergence within DMSP-related gene families. For example, TpMMT from the diatom *Thalassiosira pseudonana* is still the only characterised member of this protein family [5], and it is still difficult to predict DMSP lyase activity within the Alma family [35]. Moreover, we know that there are still important reporter genes for DMSP synthesis, transport, and catabolism to be identified (e.g., DMSP synthesis genes in DMSP-producing *Trichodesmium* cyanobacteria) [135] or dinoflagellates using the decarboxylation pathway [112], which incidentally may have been utilised by the flagellates likely responsible for the major 28 June DMSP spike at L4 (Fig. 2e). The unavoidable omissions of these genes in this analysis also led to an underestimation of certain pathways in the DMSP cycle. DMSP can be biologically transformed into various other DMSP-related compounds, such as DMSOP and gonyol, which generally occur in seawater at much lower concentrations than DMSP [25, 136] but may also contribute to DMSP cycling. These compounds were not included in this study due to limited knowledge on their key biosynthetic genes and our lack of reliable detection methods.

In summary, this study highlights the critical roles of both phototrophic microalgae and heterotrophic bacteria in DMSP synthesis and catabolism, revealing a dynamic

and at times contrasting contribution of these groups that cannot be reliably predicted from taxonomy and environmental parameters alone. Microalgae generally dominated DMSP synthesis, but it remained difficult to predict when and why bacterial production became more significant. Although bacterial DMSP demethylation consistently dominated catabolism, DMSP cleavage was also important and mostly driven by bacteria. However, sporadic high algal lyase activity occurred unpredictably, even during algal blooms. Moreover, non-conventional pathways, such as MeSH-dependent DMS production, previously considered minor contributors to the marine DMS pool, showed relatively high transcriptional activity in our study. This suggests they may play a more significant role in DMS production than previously recognised, although their occurrence remained unpredictable. Given that these findings are based on transcriptomic data, further field investigations and in situ rate measurements are warranted to quantify the actual metabolic contributions of these pathways. Prediction of the microbes and pathways potentially driving the synthesis and cycling of major organosulfur compounds was enabled by integrating process monitoring with metatranscriptomics and comprehensive molecular markers analysis. Given the considerable variability in microbial sulfur cycling revealed here at a single coastal site during one spring-summer bloom, it is essential to conduct similar studies across diverse marine waters and sediments to develop a better understanding of marine microbial organosulfur cycling.

Data availability

Raw reads of metagenomes, 16S rRNA gene amplicons, and metatranscriptomes are available at NCBI under the project accessions PRJNA901156, PRJNA901154,

and PRJNA901170, respectively. All source data used in this work are available at Zenodo (https://doi.org/10.5281/zenodo.19770266).

Funding

J.D.T. acknowledges support from the NERC grants NE/P012671, NE/S001352, NE/V000756, NE/X000990, the Leverhulme trust (RPG-2020-413) and the International Collaboration Fund, National Science Foundation China. **X-Y.Z.** and **Q.M.** acknowledge support from the Chinese Scholarship Committee. **F.E.H.** acknowledges support from the NERC grants NE/P012930/1, NE/X001075/1 and NE/W009307/1. **R.A.** acknowledges support from NERC grant NE/P012930/1. **J.D.T.** and **D.J.L-S.** acknowledge support from NERC grant NE/X014428. **J.C-O.** acknowledges project CNS2023-144462 funded by the MICIU/AEI /10.13039/501100011033 and EU NextGenerationEU/PRTR.

Acknowledgements

We are grateful for the support from the crew and scientific sampling team of the Plymouth Quest for their support in the collection of water samples for the seasonal study at station L4 of the Western Channel Observatory, which is funded by the Natural Environment Research Council (NERC) grant NE/R015953/1. We acknowledge Gill Malin for her great help in the writing of the NERC grant NE/P012671 that supported this work.

Author contributions

J.D.T., **X-Y.Z., R.A.** and **F.E.H.** conceived and designed all experiments, analysed the data, and wrote the paper. **R.A.** and **F.E.H.** collected the water samples, measured the DMSPp/DMS concentrations, and quantified the DMSPp production rates. **Q.M.** performed the DNA extraction. **X-Y.Z.** did the RNA extraction, analysed all the data, and prepared figures and tables. **J.C-O.** cultured the *Synechococcus* strains and **A.R.J.C.** measured their intracellular DMSP concentrations. **B.W.** measured the Chl-a concentrations. **E.M.S.W.** measured the nutrients. **G.A.T.** did the flow cytometry analysis. **C.E.W.** did the microalgae enumeration by microscopy. **D.J.L-S., L.H., G-P.Y., O.C., G.M. and X-H.Z.** performed critical revision of the manuscript. All authors edited and approved the manuscript.

Conflicts of interest

The authors declare that they have no competing interests.

References

1. Carrión O, Zhu X-Y, Williams BT *et al.* Molecular discoveries in microbial DMSP synthesis. In: Poole RK, Kelly DJ (eds.), *Advances in Microbial Physiology*. Amsterdam: Elsevier Science, 2023, 59-116.
2. Galí M, Devred E, Levasseur M *et al.* A remote sensing algorithm for planktonic dimethylsulfoniopropionate (DMSP) and an analysis of global patterns. *Remote Sens Environ* 2015**;**171:171-84 10.1016/j.rse.2015.10.012
3. Curson ARJ, Williams BT, Pinchbeck BJ *et al.* DSYB catalyses the key step of dimethylsulfoniopropionate biosynthesis in many phytoplankton. *Nat Microbiol* 2018**;**3:430-39 10.1038/s41564-018-0119-5
4. Wang J, Curson ARJ, Zhou S *et al.* Alternative dimethylsulfoniopropionate biosynthesis enzymes in diverse and abundant microorganisms. *Nat Microbiol* 2024**;**9:1-14 10.1038/s41564-024-01715-9
5. Kageyama H, Tanaka Y, Shibata A *et al.* Dimethylsulfoniopropionate biosynthesis in a diatom *Thalassiosira pseudonana*: Identification of a gene encoding MTHB-methyltransferase. *Arch Biochem Biophys* 2018**;**645:100-06 10.1016/j.abb.2018.03.019

6. Curson ARJ, Liu J, Bermejo Martínez A *et al.* Dimethylsulfoniopropionate biosynthesis in marine bacteria and identification of the key gene in this process. *Nat Microbiol* 2017;2:17009 10.1038/nmicrobiol.2017.9

7. Williams BT, Cowles K, Bermejo Martínez A *et al.* Bacteria are important dimethylsulfoniopropionate producers in coastal sediments. *Nat Microbiol* 2019;4:1815-25 10.1038/s41564-019-0527-1

8. Keller MD, Bellows WK, Guillard RRL. Dimethyl sulfide production in marine phytoplankton. In: Saltzman ES, Cooper WJ (eds.), *Biogenic Sulfur in the Environment*. Washington D.C.: ACS Publications, 1989, 167-82.

9. McParland EL, Levine NM. The role of differential DMSP production and community composition in predicting variability of global surface DMSP concentrations. *Limnol Oceanogr* 2019;64:757-73 10.1002/lno.11076

10. Cheng H, Zhang Y, Guo Z *et al.* Microbial dimethylsulfoniopropionate cycling in deep sediment of the Mariana Trench. *Appl Environ Microbiol* 2023;89:e00251-23 10.1128/aem.00251-23

11. Song D, Zhang Y, Liu J *et al.* Metagenomic insights into the cycling of dimethylsulfoniopropionate and related molecules in the Eastern China marginal seas. *Front Microbiol* 2020;11:157 10.3389/fmicb.2020.00157

12. Zheng Y, Wang J, Zhou S *et al.* Bacteria are important dimethylsulfoniopropionate producers in marine aphotic and high-pressure environments. *Nat Commun* 2020;11:4658 10.1038/s41467-020-18434-4

13. Reisch CR, Moran MA, Whitman WB. Dimethylsulfoniopropionate-dependent demethylase (DmdA) from *Pelagibacter ubique* and *Silicibacter pomeroyi*. *J Bacteriol* 2008;190:8018-24 10.1128/jb.00770-08

14. Ruiz-González C, Galí M, Sintes E *et al.* Sunlight effects on the osmotrophic uptake of DMSP-Sulfur and Leucine by polar phytoplankton. *PLoS One* 2012;7:e45545 10.1371/journal.pone.0045545

15. Spielmeyer A, Gebser B, Pohnert G. Investigations of the uptake of dimethylsulfoniopropionate by phytoplankton. *ChemBioChem* 2011;12:2276-79 10.1002/cbic.201100416

16. Sun J, Todd JD, Thrash JC *et al.* The abundant marine bacterium *Pelagibacter* simultaneously catabolizes dimethylsulfoniopropionate to the gases dimethyl sulfide and methanethiol. *Nat Microbiol* 2016;1:16065 10.1038/nmicrobiol.2016.65

17. Vila-Costa M, Simó R, Harada H *et al.* Dimethylsulfoniopropionate uptake by marine phytoplankton. *Science* 2006;314:652-54 10.1126/science.1131043

18. Ito T, Asano Y, Tanaka Y *et al.* Regulation of biosynthesis of dimethylsulfoniopropionate and its uptake in sterile mutant of *Ulva pertusa* (Chlorophyta). *J Phycol* 2011;47:517-23 10.1111/j.1529-8817.2011.00977.x

19. Curson ARJ, Todd JD, Sullivan MJ *et al.* Catabolism of dimethylsulphoniopropionate: microorganisms, enzymes and genes. *Nat Rev Microbiol* 2011;9:849-59 10.1038/nrmicro2653

20. Sun L, Curson ARJ, Todd JD *et al.* Diversity of DMSP transport in marine bacteria, revealed by genetic analyses. *Biogeochemistry* 2012;110:121-30 10.1007/s10533-011-9666-z

21. Clifton BE, Alcolombri U, Uechi GI *et al.* The ultra-high affinity transport proteins of ubiquitous marine bacteria. *Nature* 2024;634:721-28 10.1038/s41586-024-07924-w

22. Li C-Y, Mausz MA, Murphy A *et al.* Ubiquitous occurrence of a dimethylsulfoniopropionate ABC transporter in abundant marine bacteria. *ISME J* 2023;17:579-87 10.1038/s41396-023-01375-3

23. Buchan A, González JM, Moran MA. Overview of the marine *Roseobacter* lineage. *Appl Environ Microbiol* 2005;71:5665-77 10.1128/aem.71.10.5665-5677.2005

24. Morris RM, Rappé MS, Connon SA *et al.* SAR11 clade dominates ocean surface bacterioplankton communities. *Nature* 2002;420:806-10 10.1038/nature01240

25. Thume K, Gebser B, Chen L *et al.* The metabolite dimethylsulfoxonium propionate extends the marine organosulfur cycle. *Nature* 2018;563:412-15 10.1038/s41586-018-0675-0

26. Reisch CR, Stoudemayer MJ, Varaljay VA *et al.* Novel pathway for assimilation of dimethylsulphoniopropionate widespread in marine bacteria. *Nature* 2011;473:208-11 10.1038/nature10078

27. Howard EC, Henriksen JR, Buchan A *et al.* Bacterial taxa that limit sulfur flux from the ocean. *Science* 2006;314:649-52 10.1126/science.1130657

28. Kiene RP, Linn LJ. The fate of dissolved dimethylsulfoniopropionate (DMSP) in seawater: tracer studies using ^{35}S-DMSP. *Geochim Cosmochim Acta* 2000;64:2797-810 10.1016/S0016-7037(00)00399-9

29. Carrión O, Li C-Y, Peng M *et al.* DMSOP-cleaving enzymes are diverse and widely distributed in marine microorganisms. *Nat Microbiol* 2023;8:2326-37 10.1038/s41564-023-01526-4

30. Landa M, Burns AS, Durham BP *et al.* Sulfur metabolites that facilitate oceanic phytoplankton-bacteria carbon flux. *ISME J* 2019;13:2536-50 10.1038/s41396-019-0455-3

31. Zhang S, Cao HY, Zhang N *et al.* Novel insights into dimethylsulfoniopropionate catabolism by cultivable bacteria in the Arctic Kongsfjorden. *Appl Environ Microbiol* 2022;88:e01806-21 10.1128/AEM.01806-21

32. He X-Y, Liu N-H, Liu J-Q *et al.* SAR92 clade bacteria are potentially important DMSP degraders and sources of climate-active gases in marine environments. *mBio* 2023;14:e01467-23 10.1128/mbio.01467-23

33. Tanaka H, Esaki N, Soda K. Properties of L-methionine gamma-lyase from *Pseudomonas ovalis*. *Biochemistry* 1977;16:100-6 10.1021/bi00620a016

34. Zhou T, Wang J, Todd JD *et al.* Quorum sensing regulates the production of methanethiol in *Vibrio harveyi*. *Microorganisms* 2023;12:35 10.3390/microorganisms12010035

35. Alcolombri U, Ben-Dor S, Feldmesser E *et al.* Identification of the algal dimethyl sulfide–releasing enzyme: A missing link in the marine sulfur cycle. *Science* 2015;348:1466-69 10.1126/science.aab1586

36. Curson ARJ, Rogers R, Todd JD *et al.* Molecular genetic analysis of a dimethylsulfoniopropionate lyase that liberates the climate-changing gas dimethylsulfide in several marine α-proteobacteria and *Rhodobacter sphaeroides*. *Environ Microbiol* 2008;10:757-67 10.1111/j.1462-2920.2007.01499.x

37. Todd JD, Curson ARJ, Dupont CL *et al.* The *dddP* gene, encoding a novel enzyme that converts dimethylsulfoniopropionate into dimethyl sulfide, is widespread in ocean metagenomes and marine bacteria and also occurs in some Ascomycete fungi. *Environ Microbiol* 2009;11:1376-85 10.1111/j.1462-2920.2009.01864.x

38. Todd JD, Curson ARJ, Kirkwood M *et al.* DddQ, a novel, cupin-containing, dimethylsulfoniopropionate lyase in marine roseobacters and in uncultured marine bacteria. *Environ Microbiol* 2011;13:427-38 10.1111/j.1462-2920.2010.02348.x

39. Wang S-Y, Zhang N, Teng Z-J *et al.* A new dimethylsulfoniopropionate lyase of the cupin superfamily in marine bacteria. *Environ Microbiol* 2023;25:1238-49 10.1111/1462-2920.16355

40. Todd JD, Kirkwood M, Newton-Payne S *et al.* DddW, a third DMSP lyase in a model Roseobacter marine bacterium, *Ruegeria pomeroyi* DSS-3. *ISME J* 2012;6:223-26 10.1038/ismej.2011.79

41. Curson ARJ, Sullivan MJ, Todd JD *et al.* DddY, a periplasmic dimethylsulfoniopropionate lyase found in taxonomically diverse species of Proteobacteria. *ISME J* 2011;5:1191-200 10.1038/ismej.2010.203

42. Todd JD, Rogers R, Li YG *et al.* Structural and regulatory genes required to make the gas dimethyl sulfide in bacteria. *Science* 2007;315:666-69 10.1126/science.1135370

43. Li C-Y, Wang X-J, Chen X-L *et al.* A novel ATP dependent dimethylsulfoniopropionate lyase in bacteria that releases dimethyl sulfide and acryloyl-CoA. *Elife* 2021;10:e64045 10.7554/eLife.64045

44. Hopkins FE, Archer SD, Bell TG *et al.* The biogeochemistry of marine dimethylsulfide. *Nat Rev Earth Environ* 2023;4:361-76 10.1038/s43017-023-00428-7

45. Teng Z-J, Wang P, Chen X-L *et al.* Acrylate protects a marine bacterium from grazing by a ciliate predator. *Nat Microbiol* 2021;6:1351-56 10.1038/s41564-021-00981-1

46. Carrion O, Curson ARJ, Kumaresan D *et al.* A novel pathway producing dimethylsulphide in bacteria is widespread in soil environments. *Nat Commun* 2015;6:6579 10.1038/ncomms7579

47. Li CY, Cao HY, Wang Q *et al.* Aerobic methylation of hydrogen sulfide to dimethylsulfide in diverse microorganisms and environments. *ISME J* 2023;17:1184-93 10.1038/s41396-023-01430-z

48. Zhang Y, Sun C, Guo Z *et al.* An *S*-methyltransferase that produces the climate-active gas dimethylsulfide is widespread across diverse marine bacteria. *Nat Microbiol* 2024;9:2614-25 10.1038/s41564-024-01788-6

49. Guo R, Guo Z, Zhou Y *et al.* Two novel *S*-methyltransferases confer dimethylsulfide production in Actinomycetota. *Adv Sci* 2025:e10141 10.1002/advs.202510141

50. Bilous PT, Weiner JH. Molecular cloning and expression of the *Escherichia coli* dimethyl sulfoxide reductase operon. *J Bacteriol* 1988;170:1511-8 10.1128/jb.170.4.1511-1518.1988

51. Bilous PT, Cole ST, Anderson WF *et al.* Nucleotide sequence of the dmsABC operon encoding the anaerobic dimethylsulphoxide reductase of *Escherichia coli*. *Mol Microbiol* 1988;2:785-95 10.1111/j.1365-2958.1988.tb00090.x

52. McEwan AG, Ferguson SJ, Jackson JB. Purification and properties of dimethyl sulphoxide reductase from *Rhodobacter capsulatus*. A periplasmic molybdoenzyme. *Biochem J* 1991;274:305-07 10.1042/bj2740305

53. Gon S, Patte JC, Mejean V *et al.* The *torYZ* (*yecK bisZ*) operon encodes a third respiratory trimethylamine N-oxide reductase in *Escherichia coli*. *J Bacteriol* 2000;182:5779-86 10.1128/JB.182.20.5779-5786.2000

54. Horinouchi M, Yoshida T, Nojiri H *et al.* Polypeptide requirement of multicomponent monooxygenase DsoABCDEF for dimethyl sulfide oxidizing activity. *Biosci Biotechnol Biochem* 1999;63:1765-71 10.1271/bbb.63.1765

55. McDevitt CA, Hanson GR, Noble CJ *et al.* Characterization of the redox centers in dimethyl sulfide dehydrogenase from *Rhodovulum sulfidophilum*. *Biochemistry* 2002;41:15234-44 10.1021/bi026221u

56. Chen Y, Patel NA, Crombie A *et al.* Bacterial flavin-containing monooxygenase is trimethylamine monooxygenase. *P Natl Acad Sci USA* 2011;108:17791-96 10.1073/pnas.1112928108

57. Boden R, Borodina E, Wood AP *et al.* Purification and characterization of dimethylsulfide monooxygenase from *Hyphomicrobium sulfonivorans*. *J Bacteriol* 2011;193:1250-58 10.1128/Jb.00977-10

58. Cao Q, Liu X, Wang Q *et al.* Rhodobacteraceae methanethiol oxidases catalyze methanethiol degradation to produce sulfane sulfur other than hydrogen sulfide. *mBio* 2024;15:e02907-23 10.1128/mbio.02907-23

59. O'Brien J, Focardi A, Deschaseaux ESM *et al.* Microbial dimethylsulfoniopropionate (DMSP) cycling in the ultraoligotrophic eastern Indian Ocean. *Deep Sea Res Part II* 2022;206:105195 10.1016/j.dsr2.2022.105195

60. O'Brien J, McParland EL, Bramucci AR *et al.* The microbiological drivers of temporally dynamic dimethylsulfoniopropionate cycling processes in Australian coastal shelf waters. *Front Microbiol* 2022;13:894026 10.3389/fmicb.2022.894026

61. Liu J, Zhang Y, Liu J *et al.* Bacterial dimethylsulfoniopropionate biosynthesis in the East China Sea. *Microorganisms* 2021;9:657 10.3390/microorganisms9030657

62. Teng Z-J, Qin Q-L, Zhang W *et al.* Biogeographic traits of dimethyl sulfide and dimethylsulfoniopropionate cycling in polar oceans. *Microbiome* 2021;9:207 10.1186/s40168-021-01153-3

63. Zhang Y, Sun K, Sun C *et al.* Dimethylsulfoniopropionate biosynthetic bacteria in the subseafloor sediments of the South China Sea. *Front Microbiol* 2021;12:731524 10.3389/fmicb.2021.731524

64. McEvoy AJ, Atkinson A, Airs RL *et al.* The Western Channel Observatory: a century of physical, chemical and biological data compiled from pelagic and benthic habitats in the western English Channel. *Earth Syst Sci Data* 2023;15:5701-37 10.5194/essd-15-5701-2023

65. Welschmeyer NA. Fluorometric analysis of Chlorophyll-a in the presence of Chlorophyll-b and pheopigments. *Limnol Oceanogr* 1994;39:1985-92 10.4319/lo.1994.39.8.1985

66. Tarran GA, Bruun JT. Nanoplankton and picoplankton in the Western English Channel: abundance and seasonality from 2007-2013. *Prog Oceanogr* 2015;137:446-55 10.1016/j.pocean.2015.04.024

67. Widdicombe CE, Eloire D, Harbour D *et al.* Long-term phytoplankton community dynamics in the Western English Channel. *J Plankton Res* 2010;32:643-55 10.1093/plankt/fbp127

68. Menden-Deuer S, Lessard EJ. Carbon to volume relationships for dinoflagellates, diatoms, and other protist plankton. *Limnol Oceanogr* 2000;45:569-79 10.4319/lo.2000.45.3.0569

69. Archer SD, Kimmance SA, Stephens JA *et al.* Contrasting responses of DMS and DMSP to ocean acidification in Arctic waters. *Biogeosciences* 2013;10:1893-908 10.5194/bg-10-1893-2013

70. Hopkins FE, Archer SD. Consistent increase in dimethyl sulfide (DMS) in response to high CO in five shipboard bioassays from contrasting NW European waters. *Biogeosciences* 2014;11:4925-40 10.5194/bg-11-4925-2014

71. Stefels J, Dacey JWH, Elzenga JTM. In vivo DMSP-biosynthesis measurements using stable-isotope incorporation and proton-transfer-reaction mass spectrometry (PTR-MS). *Limnol Oceanogr-Meth* 2009;7:595-611 10.4319/lom.2009.7.595

72. Apprill A, McNally S, Parsons R *et al.* Minor revision to V4 region SSU rRNA 806R gene primer greatly increases detection of SAR11 bacterioplankton. *Aquat Microb Ecol* 2015;75:129-37 10.3354/ame01753

73. Walters W, Hyde ER, Berg-Lyons D *et al.* Improved bacterial 16S rRNA Gene (V4 and V4-5) and fungal Internal transcribed spacer marker gene primers for microbial community surveys. *Msystems* 2016;1:10-1128 10.1128/mSystems.00009-15

74. Chen SF, Zhou YQ, Chen YR *et al.* fastp: an ultra-fast all-in-one FASTQ preprocessor. *Bioinformatics* 2018;34:884-90 10.1093/bioinformatics/bty560

75. Kopylova E, Noe L, Touzet H. SortMeRNA: fast and accurate filtering of ribosomal RNAs in metatranscriptomic data. *Bioinformatics* 2012;28:3211-7 10.1093/bioinformatics/bts611

76. Li D, Luo R, Liu C *et al.* MEGAHIT v1.0: a fast and scalable metagenome assembler driven by advanced methodologies and community practices. *Methods* 2016;102:3-11 10.1016/j.ymeth.2016.02.020

77. Hyatt D, Chen G-L, LoCascio PF *et al.* Prodigal: prokaryotic gene recognition and translation initiation site identification. *BMC Bioinf* 2010;11:1-11 10.1186/1471-2105-11-119

78. Rho M, Tang H, Ye Y. FragGeneScan: predicting genes in short and error-prone reads. *Nucleic Acids Res* 2010;38:e191 10.1093/nar/gkq747

79. Fu L, Niu B, Zhu Z *et al.* CD-HIT: accelerated for clustering the next-generation sequencing data. *Bioinformatics* 2012;28:3150-2 10.1093/bioinformatics/bts565

80. Steinegger M, Soding J. MMseqs2 enables sensitive protein sequence searching for the analysis of massive data sets. *Nat Biotechnol* 2017;35:1026-28 10.1038/nbt.3988

81. Chaumeil PA, Mussig AJ, Hugenholtz P *et al.* GTDB-Tk: a toolkit to classify genomes with the genome taxonomy database. *Bioinformatics* 2019;36:1925-7 10.1093/bioinformatics/btz848

82. Krinos AI, Hu SK, Cohen NR *et al.* EUKulele: Taxonomic annotation of the unsung eukaryotic microbes. *J Open Source Softw* 2020;6:2817 10.21105/joss.02817

83. Aroney STN, Newell RJP, Nissen JN *et al.* CoverM: read alignment statistics for metagenomics. *Bioinformatics* 2025;41:btaf147 10.1093/bioinformatics/btaf147

84. Milanese A, Mende DR, Paoli L *et al.* Microbial abundance, activity and population genomic profiling with mOTUs2. *Nat Commun* 2019;10:1014 10.1038/s41467-019-08844-4

85. Eddy SR. Accelerated profile HMM searches. *PLoS Comput Biol* 2011;7:e1002195 10.1371/journal.pcbi.1002195

86. Bolyen E, Rideout JR, Dillon MR *et al.* Reproducible, interactive, scalable and extensible microbiome data science using QIIME 2. *Nat Biotechnol* 2019;37:852-57 10.1038/s41587-019-0209-9

87. Quast C, Pruesse E, Yilmaz P *et al.* The SILVA ribosomal RNA gene database project: improved data processing and web-based tools. *Nucleic Acids Res* 2013;41:D590-D96 10.1093/nar/gks1219

88. Gruber-Vodicka HR, Seah BKB, Pruesse E. phyloFlash: rapid small-subunit rRNA profiling and targeted assembly from metagenomes. *Msystems* 2020;5:e00920-20 10.1128/mSystems.00920-20

89. Langmead B, Salzberg SL. Fast gapped-read alignment with Bowtie 2. *Nat Methods* 2012;9:357-9 10.1038/nmeth.1923

90. Murali A, Bhargava A, Wright ES. IDTAXA: a novel approach for accurate taxonomic classification of microbiome sequences. *Microbiome* 2018;6:140 10.1186/s40168-018-0521-5

91. Guillou L, Bachar D, Audic S *et al.* The Protist Ribosomal Reference database (PR2): a catalog of unicellular eukaryote small sub-unit rRNA sequences with curated taxonomy. *Nucleic Acids Res* 2012;41:D597-D604 10.1093/nar/gks1160

92. Wood DE, Lu J, Langmead B. Improved metagenomic analysis with Kraken 2. *Genome Biol* 2019;20:257 10.1186/s13059-019-1891-0

93. Liu C, Cui Y, Li X *et al.* microeco: an R package for data mining in microbial community ecology. *FEMS Microbiol Ecol* 2021;97:fiaa255 10.1093/femsec/fiaa255

94. Pan S, Zhao XM, Coelho LP. SemiBin2: self-supervised contrastive learning leads to better MAGs for short- and long-read sequencing. *Bioinformatics* 2023;39:i21-i29 10.1093/bioinformatics/btad209

95. Olm MR, Brown CT, Brooks B *et al.* dRep: a tool for fast and accurate genomic comparisons that enables improved genome recovery from metagenomes through de-replication. *ISME J* 2017;11:2864-68 10.1038/ismej.2017.126

96. Parks DH, Imelfort M, Skennerton CT *et al.* CheckM: assessing the quality of microbial genomes recovered from isolates, single cells, and metagenomes. *Genome Res* 2015;25:1043-55 10.1101/gr.186072.114

97. Xie J, Chen Y, Cai G *et al.* Tree Visualization By One Table (tvBOT): a web application for visualizing, modifying and annotating phylogenetic trees. *Nucleic Acids Res* 2023;51:W587-W92 10.1093/nar/gkad359

98. Seemann T. Prokka: rapid prokaryotic genome annotation. *Bioinformatics* 2014;30:2068-9 10.1093/bioinformatics/btu153

99. Kanehisa M, Sato Y, Morishima K. BlastKOALA and GhostKOALA: KEGG tools for functional characterization of genome and metagenome sequences. *J Mol Biol* 2016;428:726-31 10.1016/j.jmb.2015.11.006

100. Buchfink B, Reuter K, Drost HG. Sensitive protein alignments at tree-of-life scale using DIAMOND. *Nat Methods* 2021;18:366-68 10.1038/s41592-021-01101-x

101. Saier MH, Reddy VS, Moreno-Hagelsieb G *et al.* The Transporter Classification Database (TCDB): 2021 update. *Nucleic Acids Res* 2021;49:D461-D67 10.1093/nar/gkaa1004

102. Wilson WH, Carr NG, Mann NH. The effect of phosphate status on the kinetics of cyanophage infection in the oceanic cyanobacterium *Synechococcus* sp WH7803. *J Phycol* 1996;32:506-16 10.1111/j.0022-3646.1996.00506.x

103. Christie-Oleza JA, Sousoni D, Lloyd M *et al.* Nutrient recycling facilitates long-term stability of marine microbial phototroph-heterotroph interactions. *Nat Microbiol* 2017;2:1-10 10.1038/nmicrobiol.2017.100

104. Dedman CJ, Christie-Oleza JA, Fernandez-Juarez V *et al.* Cell size matters: Nano- and micro-plastics preferentially drive declines of large marine phytoplankton due to co-aggregation. *J Hazard Mater* 2022;424:127488 10.1016/j.jhazmat.2021.127488

105. Lea-Smith DJ, Ortiz-Suarez ML, Lenn T *et al.* Hydrocarbons are essential for optimal cell size, division, and growth of Cyanobacteria. *Plant Physiol* 2016;172:1928-40 10.1104/pp.16.01205

106. Speeckaert G, Borges AV, Champenois W *et al.* Annual cycle of dimethylsulfoniopropionate (DMSP) and dimethylsulfoxide (DMSO) related to phytoplankton succession in the Southern North Sea. *Sci Total Environ* 2018;622-623:362-72 10.1016/j.scitotenv.2017.11.359

107. Lizotte M, Levasseur M, Law CS *et al.* Dimethylsulfoniopropionate (DMSP) and dimethyl sulfide (DMS) cycling across contrasting biological hotspots of the New Zealand subtropical front. *Ocean Sci* 2017;13:961–82 10.5194/os-13-961-2017

108. Kiene RP, Nowinski B, Esson K *et al.* Unprecedented DMSP concentrations in a massive dinoflagellate bloom in Monterey Bay, CA. *Geophys Res Lett* 2019;46:12279-88 10.1029/2019GL085496

109. Belliardo C, Koutsovoulos GD, Rancurel C *et al.* Improvement of eukaryotic protein predictions from soil metagenomes. *Sci Data* 2022;9 10.1038/s41597-022-01420-4

110. Li C-Y, Zhang D, Chen X-L *et al.* Mechanistic insights into dimethylsulfoniopropionate lyase DddY, a new member of the cupin superfamily. *J Mol Biol* 2017;429:3850-62 10.1016/j.jmb.2017.10.022

111. Li C-Y, Crack JC, Newton-Payne S *et al.* Mechanistic insights into the key marine dimethylsulfoniopropionate synthesis enzyme DsyB/DSYB. *mLife* 2022;1:114-30 10.1002/mlf2.12030

112. Uchida A, Ooguri T, Ishida T *et al.* Biosynthesis of dimethylsulfoniopropionate in *Crypthecodinium Cohnii* (Dinophyceae). In: Kiene RP, Visscher PT, Keller MD *et al.* (eds.), *Biological and environmental chemistry of DMSP and related sulfonium compounds*. Boston, MA: Springer, 1996, 97-107.

113. Archer SD, Tarran GA, Stephens JA *et al.* Combining cell sorting with gas chromatography to determine phytoplankton group-specific intracellular dimethylsulphoniopropionate. *Aquat Microb Ecol* 2011;62:109-21 10.3354/ame01464

114. Corn M, Belviso S, Partensky F *et al.* Origin and importance of picoplanktonic DMSP. In: Kiene RP, Visscher PT, Keller MD *et al.* (eds.), *Biological and environmental*

chemistry of DMSP and related sulfonium compounds. Boston, MA: Springer, 1996, 191-201.

115. Breyer E, Stix C, Kilker S *et al.* The contribution of pelagic fungi to ocean biomass. *Cell* 2025;188:3992-4002 10.1016/j.cell.2025.05.004

116. Liu X, Wang XR, Zhou F *et al.* Novel insights into dimethylsulfoniopropionate cleavage by deep subseafloor fungi. *Sci Total Environ* 2024;933:173057 10.1016/j.scitotenv.2024.173057

117. O'Brien J, McParland EL, Bramucci AR *et al.* Biogeographical and seasonal dynamics of the marine Roseobacter community and ecological links to DMSP-producing phytoplankton. *ISME Commun* 2022;2:16 10.1038/s43705-022-00099-3

118. Stefels J, Dijkhuizen L. Characteristics of DMSP-lyase in *Phaeocystis* sp. (Prymnesiophyceae). *Mar Ecol Prog Ser* 1996;131:307-13 10.3354/meps131307

119. Mohapatra BR, Rellinger AN, Kieber DJ *et al.* Comparative functional characteristics of DMSP lyases extracted from polar and temperate *Phaeocystis* species. *Aquat Biol* 2013;18:185-95 10.3354/ab00504

120. Li CY, Cao HY, Payet RD *et al.* Dimethylsulfoniopropionate (DMSP): from biochemistry to global ecological significance. *Annu Rev Microbiol* 2024;78:513-32 10.1146/annurev-micro-041222-024055

121. Herrmann J, Jaeschke W. Measurements of H_2S and SO_2 over the Atlantic Ocean. *J Atmos Chem* 1984;1:111-23 10.1007/BF00053834

122. Cutter GA, Walsh RS, de Echols CS. Production and speciation of hydrogen sulfide in surface waters of the high latitude North Atlantic Ocean. *Deep Sea Res Part II* 1999;46:991-1010 10.1016/S0967-0645(99)00013-2

123. Dixon JL, Hopkins FE, Stephens JA *et al.* Seasonal changes in microbial dissolved organic sulfur transformations in coastal waters. *Microorganisms* 2020;8:337 10.3390/microorganisms8030337

124. Broy S, Chen C, Hoffmann T *et al.* Abiotic stress protection by ecologically abundant dimethylsulfoniopropionate and its natural and synthetic derivatives: insights from *Bacillus subtilis*. *Environ Microbiol* 2015;17:2362-78 10.1111/1462-2920.12698

125. Gregory GJ, Boas KE, Boyd EF. The organosulfur compound dimethylsulfoniopropionate (DMSP) is utilized as an osmoprotectant by *Vibrio* species. *Appl Environ Microbiol* 2021;87:e02235-20 10.1128/AEM.02235-20

126. Gao XX, Chen JF, Zhai X *et al.* Driving factors of dimethylated sulfur compounds in the Pearl River Estuary and its adjacent coastal waters: The nonnegligible role of *Synechococcus*. *J Geophys Res-Oceans* 2025;130:e2024JC021764 10.1029/2024JC021764

127. Malmstrom RR, Kiene RP, Vila M *et al.* Dimethylsulfoniopropionate (DMSP) assimilation by *Synechococcus* in the Gulf of Mexico and northwest Atlantic Ocean. *Limnol Oceanogr* 2005;50:1924-31 10.4319/lo.2005.50.6.1924

128. Van Alstyne KL, Wolfe GV, Freidenburg TL *et al.* Activated defense systems in marine macroalgae: evidence for an ecological role for DMSP cleavage. *Mar Ecol Prog Ser* 2001;213:53-65 10.3354/meps213053

129. Wolfe GV, Steinke M, Kirst GO. Grazing-activated chemical defence in a unicellular marine alga. *Nature* 1997;387:894-97 10.1038/43168

130. Miller TR, Hnilicka K, Dziedzic A *et al.* Chemotaxis of *Silicibacter* sp. strain TM1040 toward dinoflagellate products. *Appl Environ Microbiol* 2004;70:4692-701 10.1128/AEM.70.8.4692-4701.2004

131. Seymour JR, Simó R, Ahmed T *et al.* Chemoattraction to dimethylsulfoniopropionate throughout the marine microbial food web. *Science* 2010;329:342-45 10.1126/science.1188418

132. Shemi A, Alcolombri U, Schatz D *et al.* Dimethyl sulfide mediates microbial predator–prey interactions between zooplankton and algae in the ocean. *Nat Microbiol* 2021;6:1357-66 10.1038/s41564-021-00971-3

133. Wohl C, Villamayor J, Gali M *et al.* Marine emissions of methanethiol increase aerosol cooling in the Southern Ocean. *Sci Adv* 2024;10:eadq2465 10.1126/sciadv.adq2465

134. Gros V, Bonsang B, Sarda-Estève R *et al.* Concentrations of dissolved dimethyl sulfide (DMS), methanethiol and other trace gases in context of microbial communities from the temperate Atlantic to the Arctic Ocean. *Biogeosciences* 2023;20:851-67 10.5194/bg-20-851-2023

135. Bucciarelli E, Ridame C, Sunda WG *et al.* Increased intracellular concentrations of DMSP and DMSO in iron-limited oceanic phytoplankton *Thalassiosira oceanica* and *Trichodesmium erythraeum*. *Limnol Oceanogr* 2013;58:1667-79 10.4319/lo.2013.58.5.1667

136. Sacks JS, Heal KR, Boysen AK *et al.* Quantification of dissolved metabolites in environmental samples through cation-exchange solid-phase extraction paired with liquid chromatography-mass spectrometry. *Limnol Oceanogr-Meth* 2022;20:683-700 10.1002/lom3.10513

Figure 1 DMSP synthesis, import and catabolism and their environmental importance in surface oceans. Microalgae and bacteria synthesise DMSP as an anti-stress, storage or signalling molecule. Once released, DMSP can be imported by marine microbes through BCCT and/or ABC (SAR11_1336 and DmpX) family transporters for its anti-stress properties and/or as a carbon and sulfur source. DMSP is degraded by diverse marine microbes through cleavage (via Ddd or Alma enzymes) or demethylation (initially via DmdA) pathways, yielding the climate-active gases DMS and MeSH, respectively. DMS is also a potent chemoattractant for marine organisms and the major

biogenic sulfur source transferred from the sea to air. DMSP cleavage can also yield acrylate, which can be used in anaerobic respiration or predator deterrence. H_2S, MeSH and DMSO are also DMS precursors. Conversely, DMS can be oxidised to DMSO or degraded to MeSH. MeSH can be degraded to sulfane sulfur (S^0). The key enzymes involved in each reaction are in blue font. CCN, Cloud condensation nuclei.

Figure 2 Variation in plankton communities, DMSPp, DMS, and Chl-a at station L4 from 23 March to 19 July 2021. a Biomass of microalgae determined by microscopy. **b** Biomass of *Synechococcus* determined by flow cytometry. **c** Biomass of heterotrophic bacteria determined by flow cytometry. **d** Prokaryotic community composition determined by 16S rRNA gene amplicon sequencing. Some samples were not subjected to amplicon sequencing. **e** DMSPp and DMS concentrations and DMSPp:Chl-a ratios are shown by line plots. DMSPp production rates in small microalgae/free-living bacteria (0.7–3 μm) versus large microalgae/particle-associated bacteria (>3 μm) are presented in stacked bar plots. The DMSPp production rates shown are 5 times the measured values. The x-axis represents the sampling dates (e.g., "3_23" indicates 23 March). Chl-a concentrations are shown as the light green area in the background.

Figure 3 Spearman correlation analyses among environmental parameters (a), and between environmental parameters and the biomass of different plankton groups (b). Spearman's rho values are shown only for significant correlations.

Figure 4 Maximum-likelihood tree of MAGs containing DMSP synthesis and catabolic genes. The lowest resolved taxonomic assignment for each MAG is shown in brackets. Genome completeness is indicated by pie charts. The copy numbers of DMSP synthesis and catabolic genes in each MAG are shown as bubble plots. Additional genes introduced in **Fig. 1** were also examined in these MAGs to illustrate their co-occurrence.

Figure 5 Relative transcript abundance of DMSP synthesis genes at station L4 in the WEC from 23 March to 19 July 2021. a Expression and order-level taxonomic profiles of all detected synthesis genes. DMSPp concentrations in corresponding samples are shown. **b** Taxonomic composition of each DMSP synthesis gene. Biological replicate counts (n) are shown in parentheses after each sample name. Pre, pre-bloom; Diatom, diatom bloom; Dinoflagellate, dinoflagellate bloom. TPM, transcripts per million reads.

Figure 6 Relative transcript abundance of genes responsible for DMSP demethylation, DMSP/H_2S/MeSH/DMSO-dependent DMS production, and DMS degradation at station L4 in the WEC from 23 March to 19 July 2021. a Expression and order-level taxonomic profiles of all detected genes. DMSPp or DMS concentrations in corresponding samples are shown. **b** Taxonomic composition of each gene. Biological replicate counts (n) are shown in parentheses after each sample name.

Figure 7 Relative transcript abundance of potential DMSP transporter genes at station L4 in the WEC from 23 March to 19 July 2021. a Expression and order-level taxonomic profiles of all detected DMSP transporter genes. DMSPp concentrations in corresponding samples are shown. **b** Taxonomic composition of each DMSP transporter gene. **c** Comparison of the expression levels of DMSP transporter (red) and catabolic (yellow) genes from the five predicted DMSP degraders at L4. Biological replicate counts (n) are shown in parentheses after each sample name.

Click here to access/download;Figure;Fig1.pdf

CCN

Increased albedo

Sulfate aerosols

MeSH

DMS

Chemotaxis

Zooplankton

Deter

Met

DSYB
DSYE
TpMMT

DMSP

DsyB
DsyG
DsyGD
MmtN

Met

Antistress
Signalling
C & S storage

Lysis and/or
export

DMSP producers

Chemotaxis

SAR11_1336
DmpX
BCCT

Chemotaxis

Antistress

DMSP importers

S^0

MtoX

Met

MegL

H_2S

Mdd

Mdd

DmoAB

Tmm
DdhABC
DsoABCDEF

DMSO

DmsA
TorZ
DorA

SH

MeSH

S

DMS

DmdD/AcuH
DmdC
DmdB
DmdA

Alma

Ddd

Antistress

Anaerobic
respiration

Acrylate
or
Acryloyl-CoA
or
3HP-CoA

Assimilation

DMSP degraders

Microalgae

Archaea

Bacteria

Fungi

Figure2

Click here to access/download;Figure;Fig2.pdf

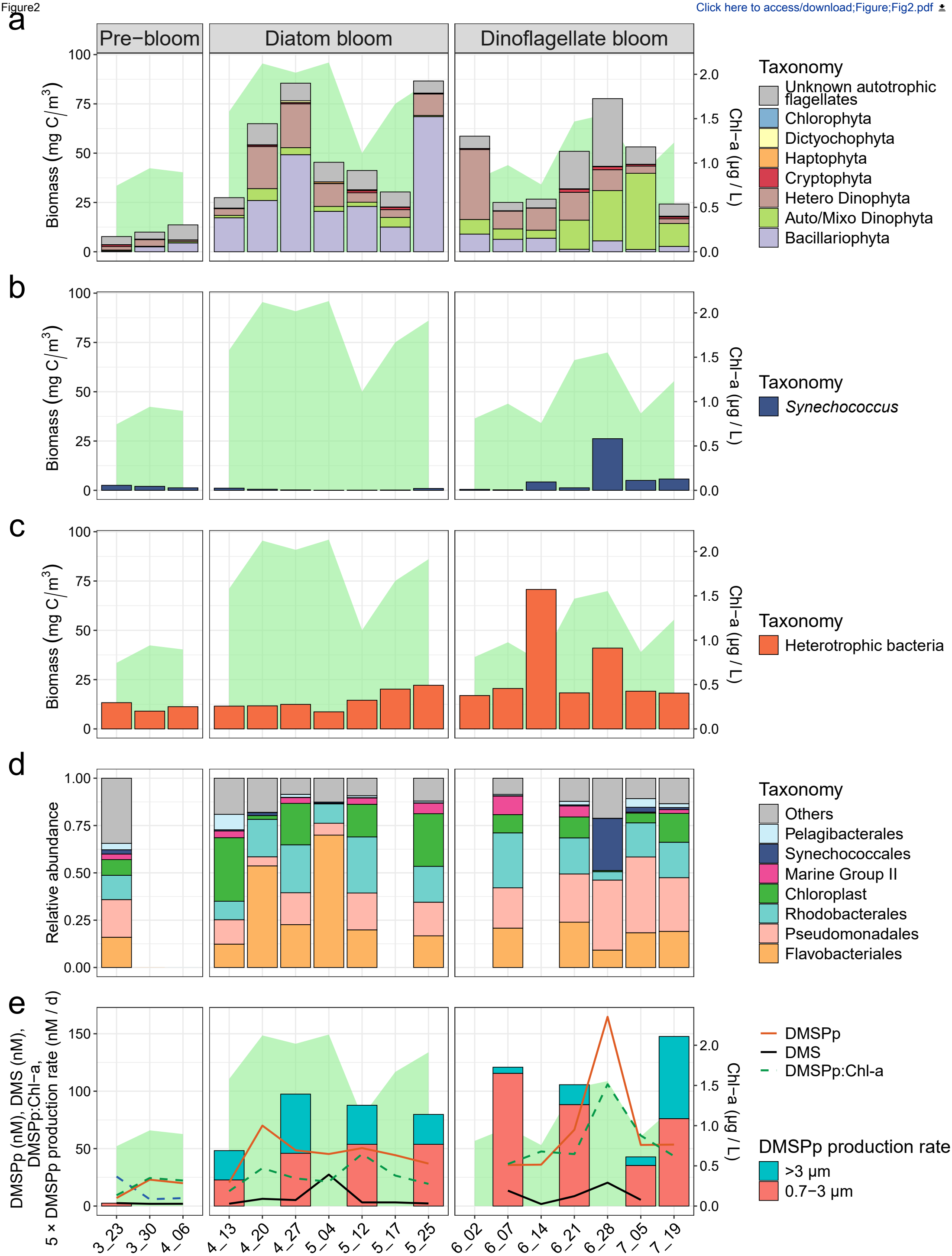

Figure3

Click here to access/download;Figure;Fig3.pdf

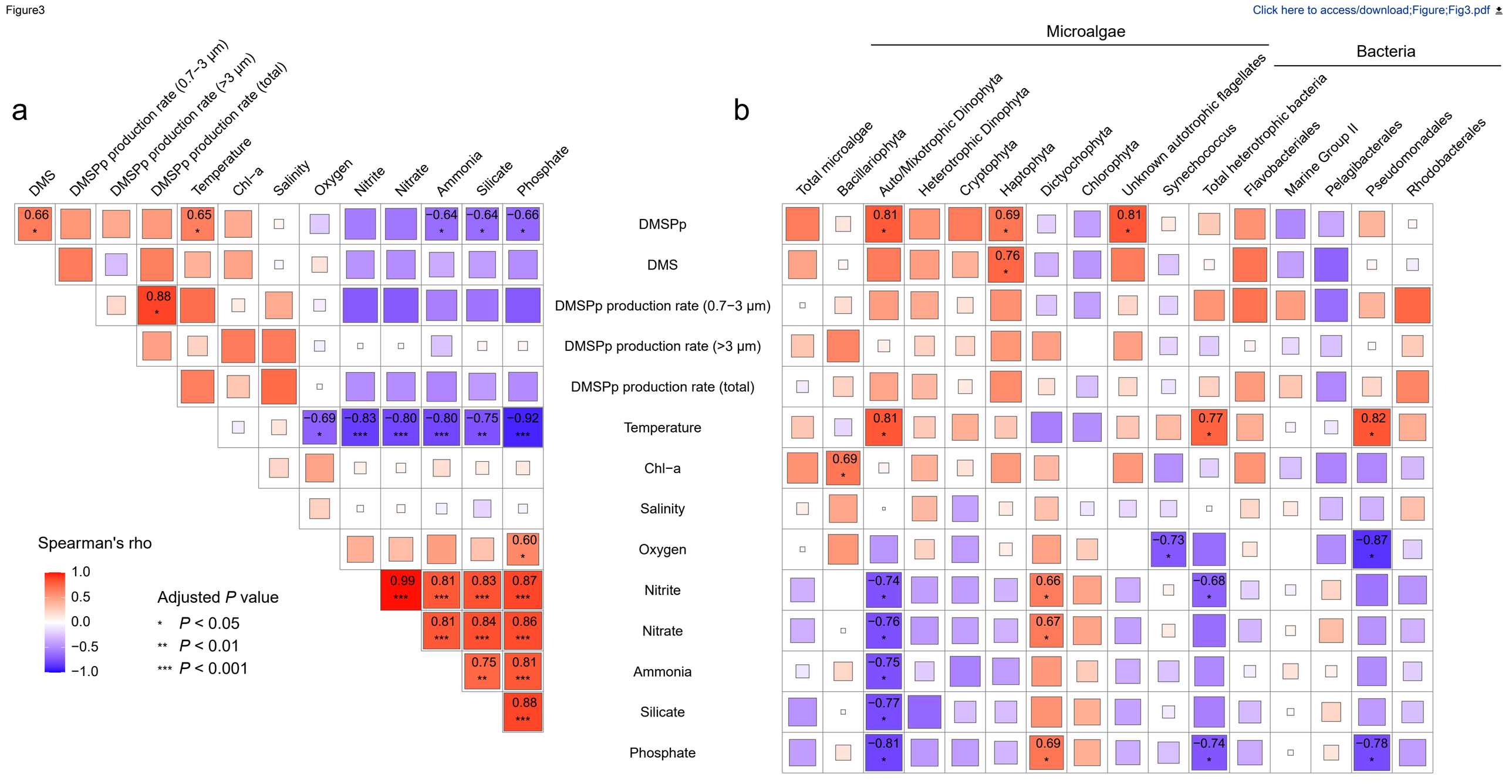

Figure4

Click here to access/download;Figure;Fig4.pdf

Figure5

Click here to access/download;Figure;Fig5.pdf

a

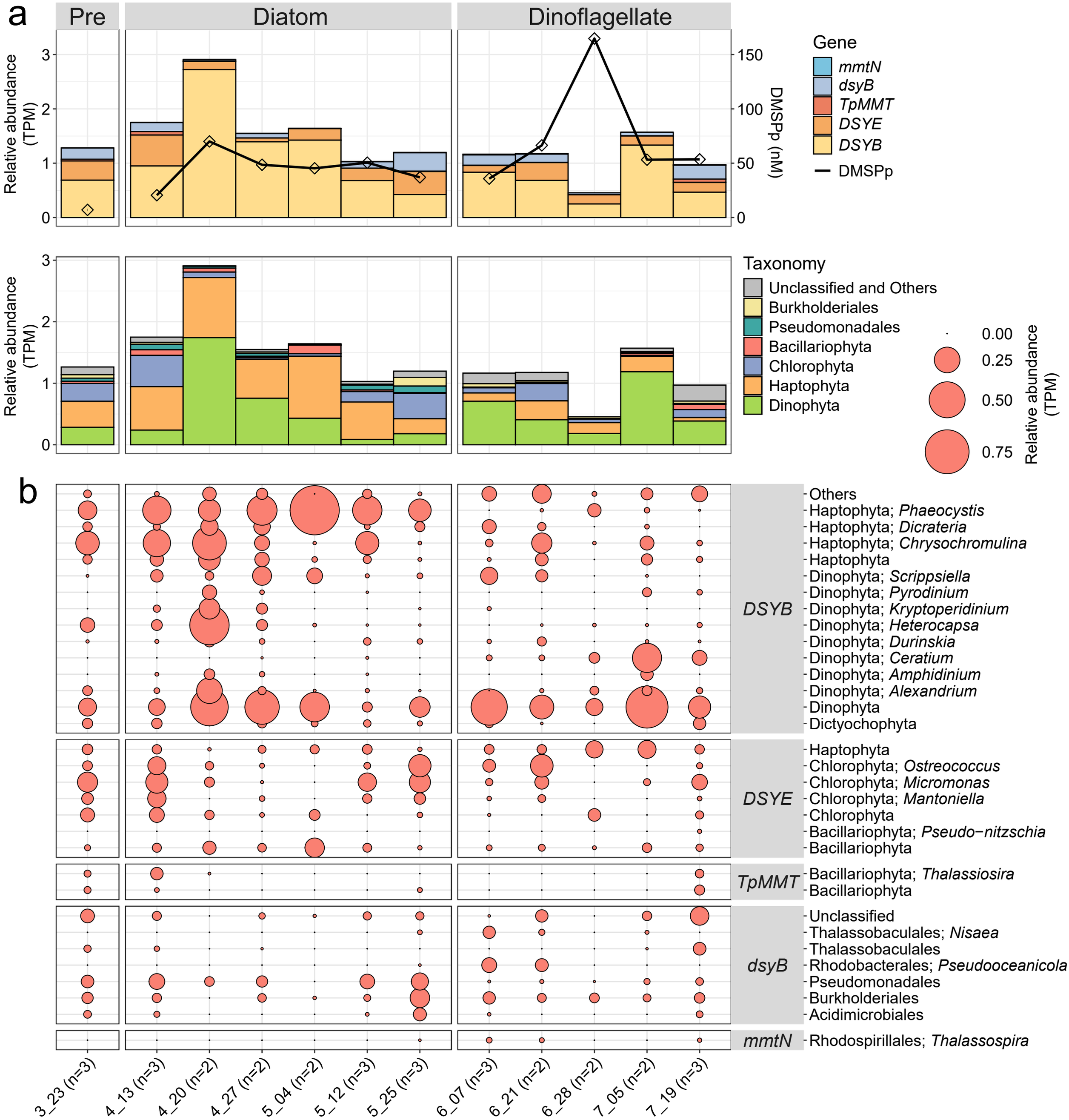

Figure6

Click here to access/download;Figure;Fig6.pdf

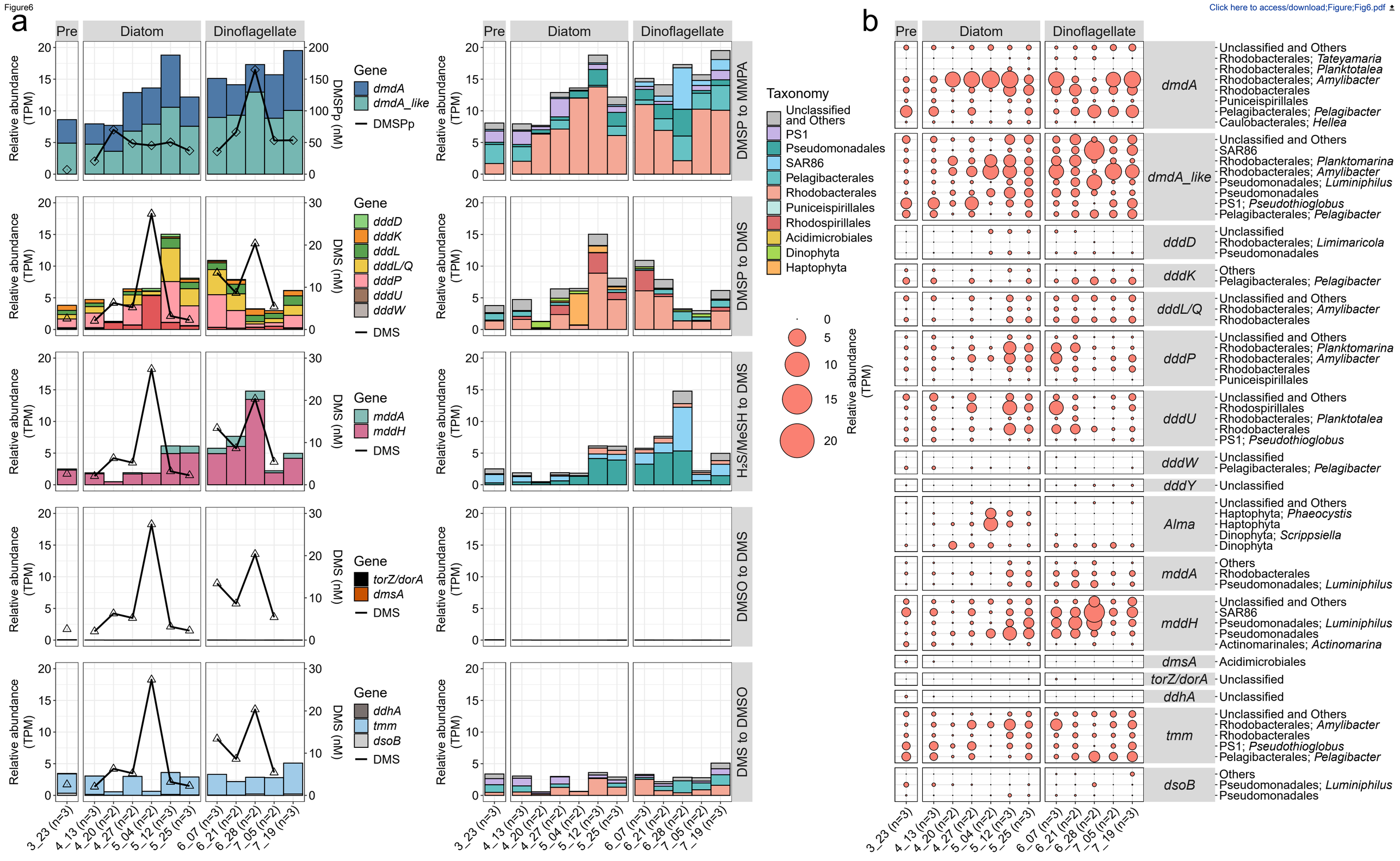

Click here to access/download;Figure;Fig7.pdf

a

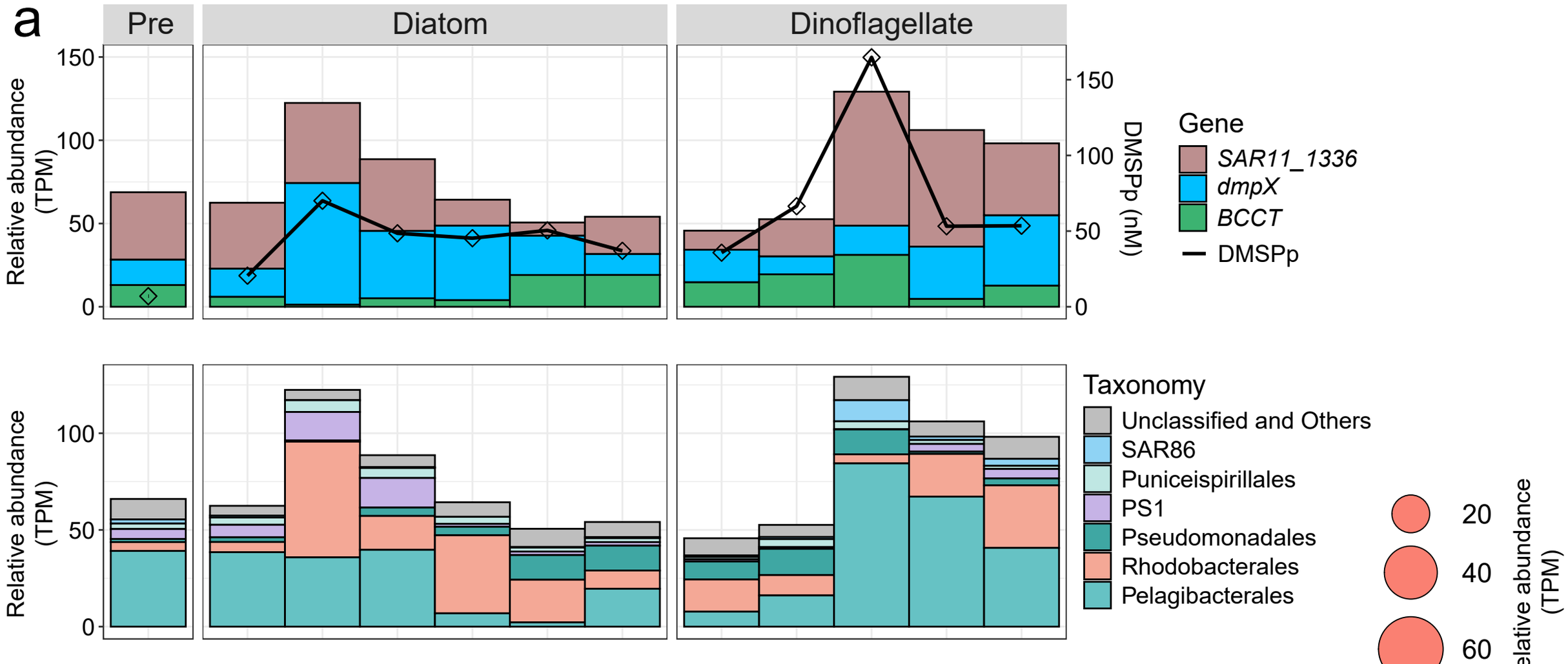

b

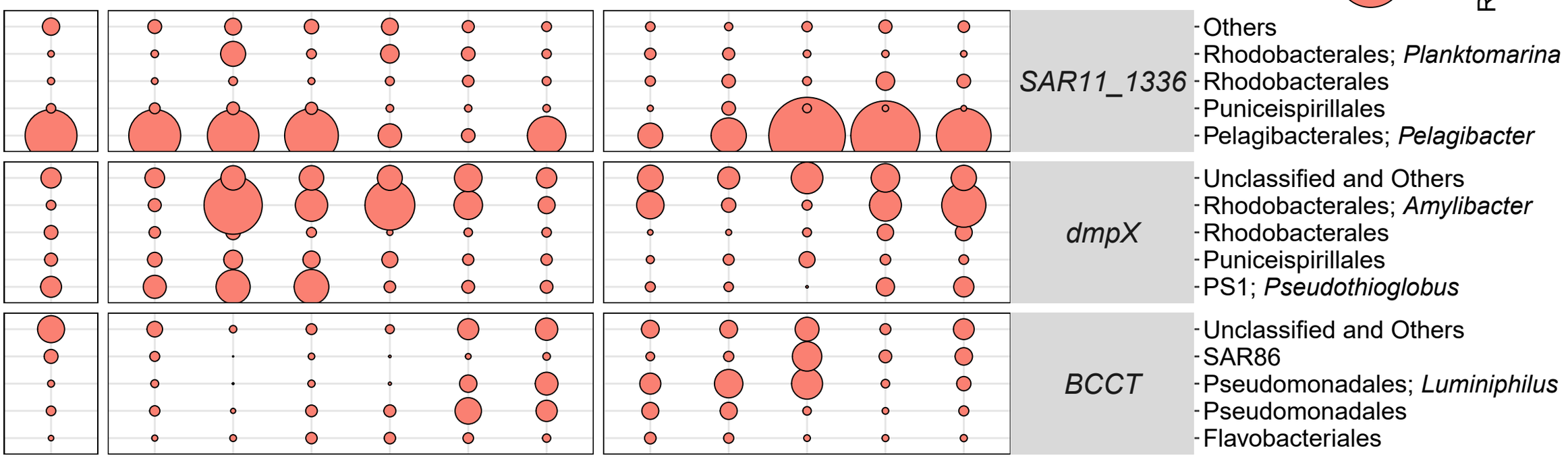

c

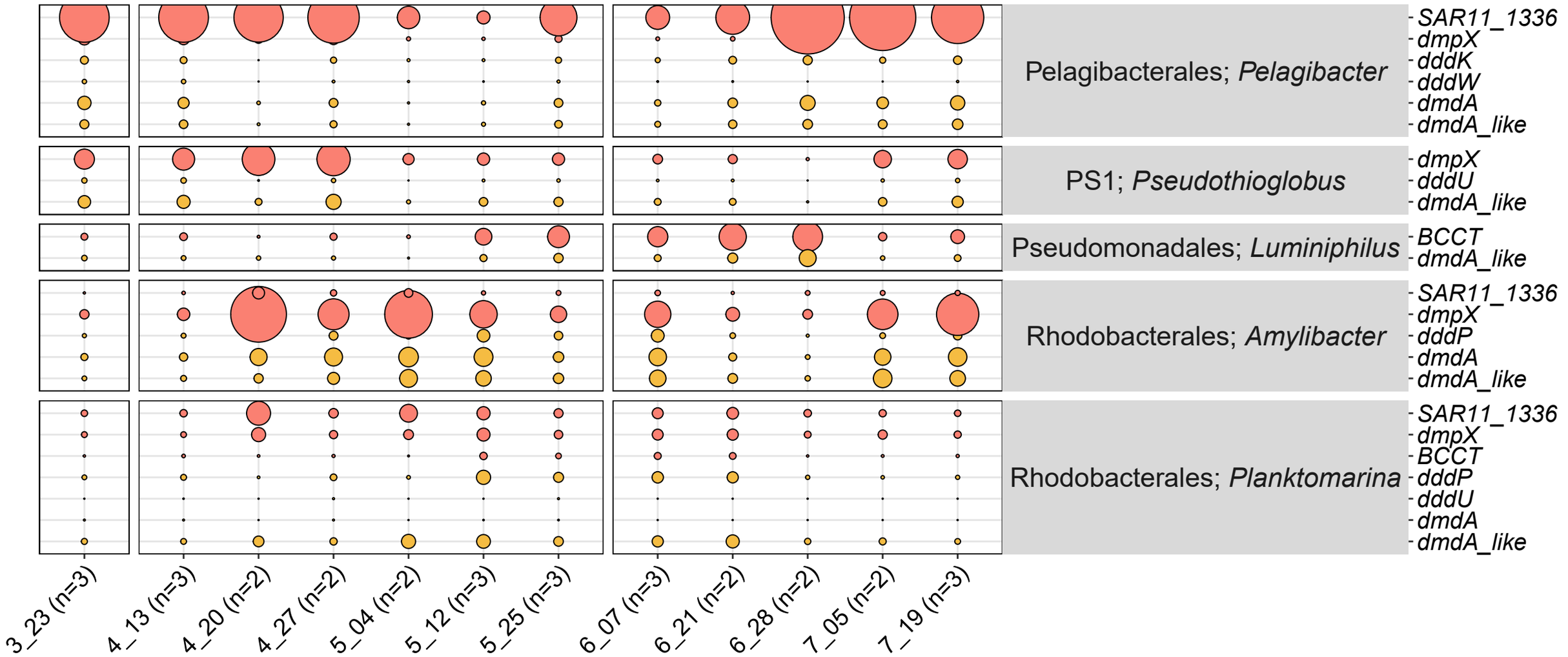

Supplementary figures

Click here to access/download
Supplemental Material
L4_Supplementary_figures.docx

Supplementary tables

Click here to access/download

Supplemental Material

L4_Supplementary_tables.xlsx